ISTANBUL TECHNICAL UNIVERSITY ★ GRADUATE SCHOOL OF SCIENCE ENGINEERING AND TECHNOLOGY

A STUDY ON MODELING THE REGIONAL IONOSPHERE USING MULTI-CONSTELLATION GNSS OBSERVATIONS FOR SINGLE-FREQUENCY PPP

Ph.D. THESIS

Mohamed Abdelazeem Mostafa MANSOUR

Department of Geomatics Engineering
Geomatics Engineering Programme

MAY 2016

ISTANBUL TECHNICAL UNIVERSITY ★ GRADUATE SCHOOL OF SCIENCE ENGINEERING AND TECHNOLOGY

A STUDY ON MODELING THE REGIONAL IONOSPHERE USING MULTI-CONSTELLATION GNSS OBSERVATIONS FOR SINGLE-FREQUENCY PPP

Ph.D. THESIS

Mohamed Abdelazeem Mostafa MANSOUR
(501122604)

Department of Geomatics Engineering

Geomatics Engineering Programme

Thesis Advisor: Prof. Dr. Rahmi Nurhan ÇELİK

Thesis Co-Advisor: Prof. Dr. Ahmed EL-RABBANY

MAY 2016

İSTANBUL TEKNİK ÜNİVERSİTESİ ★ FEN BİLİMLERİ ENSTİTÜSÜ

ÇOKLU GLOBAL UYDU KONUM BELİRLEME SİSTEMLERİNİN GÖZLEMLERİ KULLANILARAK TEK FREKANSLI PPP İÇİN BÖLGESEL İYONOSFERİK MODELLEME ÜZERİNE BİR ÇALIŞMA

DOKTORA TEZİ

Mohamed Abdelazeem Mostafa MANSOUR
(501122604)

Geomatik Mühendisliği Anabilim Dalı

Geomatik Mühendisliği Programı

Tez Danışmanı: Prof. Dr. Rahmi Nurhan ÇELİK

Tez EŞ-Danışmanı: Prof. Dr. Ahmed EL-RABBANY

MAYIS 2016

Mohamed Abdealzeem Mostafa MANSOUR, a **Ph.D.** student of ITU **Graduate School of Science Enginerring and Technology** student ID **501122604**, successfully defended the **dissertation** entitled "**A STUDY ON MODELING THE REGIONAL IONOSPHERE USING MULTI-CONSTELLATION GNSS OBSERVATIONS FOR SINGLE-FREQUENCY PPP"** which he prepared after fulfilling the requirements specified in the associated legislations, before the jury whose signatures are below.

Thesis Advisor :	**Prof. Dr. Rahmi Nurhan ÇELİK** Istanbul Technical University	.....
Thesis Co-advisor :	**Prof. Dr. Ahmed EL-RABBANY** Ryerson University, Canada	.....
Jury Members :	**Assoc. Prof. Dr. M. Tevfik ÖZLÜDEMİR** Istanbul Technical University	.....
	Assoc. Prof. Dr. Bihter EROL Istanbul Technical University	.....
	Assoc. Prof. Dr. Ersoy ARSLAN Istanbul Technical University	.....
	Prof. Dr. Doğan Uğur ŞANLI Yıldız Technical University	.....
	Prof. Dr. Şenol Hakan KUTOĞLU Bülent Ecevit University	.....

Date of Submission : 30 March 2016
Date of Defense : 5 May 2016

To the soul of my father, and to
my dearest mother and family

FOREWORD

All gratitude is to almighty ALLLAH who guided me and granted me the health, strength, the patience and the opportunity to complete my Ph.D. thesis at Istanbul Technical University after almost three years of hard works.

I would like to thank my supervisor Prof. Dr. Rahmi Nurhan ÇELİK for his supervision, his support, continuous encouragement, providing the facilities and his sincere advices during the preparation of the thesis.

Also, I would like to express my thanks to my supervisor Prof. Dr. Ahmed EL-RABBANY for his professional supervision, valuable comments, precious ideas during my study, giving me the opportunity to spend 12 months in Civil Engineering Department, Ryerson University and providing the facilities during my visit to Ryerson university.

In addition, I give my appreciation and thanks to the jury members, Dr. M. Tevfik ÖZLÜDEMİR, Prof. Dr. Doğan Uğur ŞANLI, Dr. Bihter EROL, Dr. Ersoy ARSLAN and Prof. Dr. Şenol Hakan KUTOĞLU for their dedicating time to review my thesis.

I also acknowledge the Ministry of Higher Education in Egypt and the Turkish Government for their support to me during my study in Turkey and Canada.

My thanks also to all those who helped me, in one way or another, to achieve my Ph.D. thesis.

This Ph.D. thesis is achieved under the joint Ph.D. supervision program between ITU and Ryerson University, Canada.

Finally, I acknowledge who will cite my thesis as follows:

Abdelazeem, M. (2016). A Study On Modeling The Regional Ionosphere Using Multi-Constellation GNSS Observations For Single-Frequency PPP. *Ph.D. Thesis*, Istanbul Technical University, Turkey.

May 2016 Mohamed A. M. MANSOUR

TABLE OF CONTENTS

Page

LIST OF TABLES

Page

LIST OF FIGURES

Page

A STUDY ON MODELING THE REGIONAL IONOSPHERE USING MULTI-CONSTELLATION GNSS OBSERVATIONS FOR SINGLE-FREQUENCY PPP

SUMMARY

Currently, the use of single-frequency Precise Point Positioning (PPP) technique for precise applications is limited by the effect of the ionospheric delay. For this purpose, a number of models have been developed for post processing and real-time applications. In addition, a number of international organizations have developed ionospheric correction products, including the International Global Navigation Satellite Systems (GNSS) Service (IGS). Unfortunately, however, those models and products have limited accuracy or spatiotemporal resolution, which may not be adequate for single-frequency PPP applications. To overcome this problem, this study introduces the development of regional ionospheric error correction models for single-frequency PPP users in Europe.

A Regional Ionospheric Model (RIM) over Europe is firstly developed. The proposed model has a spatial and temporal resolutions of 1º×1º and 15 minutes, respectively. GNSS observations from a regional network consisting of 60 IGS and EUREF reference stations are processed using the Bernese 5.2 software to extract the Vertical Total Electron Content (VTEC) values. To validate the newly proposed RIM, the single-frequency PPP accuracy and convergence time for another set of stations are estimated and compared with those of the IGS Global Ionospheric Maps (IGS-GIM) counterparts in three different days. The ionosphere-free dual frequency PPP is used as reference. The findings reveal that the proposed RIM accelerates the convergence time and enhances the positioning accuracy by about 20%, 45% and 45% for the horizontal, height and 3D components, respectively, in comparison with the IGS-GIM model.

In addition, a Real-Time Regional Ionospheric Model (RT-RIM) is developed using the IGS Real-Time Service (IGS-RTS) precise satellite orbit and clock products. The spatial and temporal resolutions of the proposed model are also 1º×1º and 15 minutes, respectively. In order to produce the real-time VTECs, Global Positioning System (GPS) observations from a regional network consisting of 60 IGS and EUREF reference stations are processed using the Bernese 5.2 software. The newly proposed RT-RIM is validated for PPP applications for another set of stations in three successive days. The PPP convergence time and positioning accuracy obtained through the RT-RIM is assessed and compared with those obtained through the IGS-GIM model. The ionosphere-free dual frequency PPP is used as reference. It is shown that the developed RT-RIM speeds up the convergence time. Moreover, the PPP accuracy is improved by about 40%, 55% and 40% for the 2D, height and 3D components, respectively, with respect to the IGS-GIM counterparts.

To precisely model the ionosphere TEC, a Multi-constellation GNSS Receiver Differential Code Bias (MGR-DCB) estimation model is developed. The proposed model estimates the receiver DCBs for the GPS, Galileo and BeiDou signals using the ionosphere-corrected pseudoranges differences. A regional ionospheric model is developed in order to remove the ionospheric errors from the pseudorange differences. The proposed RIM has a spatial and temporal resolutions of $1^{o}\times1^{o}$ and 15 minutes, respectively. To validate the developed MGR-DCB model, the receiver DCBs for three IGS Multi-GNSS Experiment (IGS-MGEX) stations are obtained for three different days. The estimated DCB values are compared with the published MGEX values. The results show that the agreement between the estimated DCBs and the MGEX is less than 1 ns for both of the mean difference and Root Mean Square Error (RMSE) values. Moreover, the VTEC values are computed from the combined GPS, Galileo and BeiDou measurements and compared with the IGS-GIM counterparts. It is shown that the computed VETC values have good agreement with the IGS-GIM counterparts with mean difference and RMSE values less than 1 Total Electron Content Unit (TECU).

ÇOKLU GLOBAL UYDU KONUM BELİRLEME SİSTEMLERİNİN GÖZLEMLERİ KULLANILARAK TEK FREKANSLI PPP İÇİN BÖLGESEL İYONOSFERİK MODELLEME ÜZERİNE BİR ÇALIŞMA

ÖZET

İyonosfer Dünya'nın yüzeyi üzerinde yaklaşık 50-1000 km mesafede bulunan tabakadır. Bu tabaka sırasıyla D-tabakası, E-tabakası, F1-tabakası ve F2-tabakası olmak üzere dört ana katmandan oluşur. İyonosfer, uydu ile alıcı arasındaki görüş-hattı (line-of-sight) boyunca toplam elektronların sayısı olan Toplam Elektron İçeriği (Total Electron Content- TEC) tarafından miktarı belirlenmiş serbestçe yüklü elektronların bulunduğu bir bölgedir. Toplam elektron içeriği, günlük, aylık, sezonluk ve tahmini 11 yıllık güneş döngüşünün varyasyonlarını içerir. Aynı zamanla coğrafi konuma göre değişir.

Dünya'nın iyonosfer tabakası dağıtıcı bir ortamdır. Bu, sinyal yayılım hızının frekansa bağımlı olduğu anlamına gelir. İyonosfer ışık hızının ötesinde faz gözlemlerini hızlandırır ancak kod gözlemlerini geciktirir. Ayrıca, faz ve genlik sintilasyonuna sebep olur. İyonosferik gecikme, yüksek ionosferik faaliyetler sırasında bir metreden daha az bir düzeyden onlarca metreye kadar değişim göstermektedir. Bu nedenle, hem global hem de bölgesel ölçekte iyonosfer toplam elektron içeriğinin prezisyonlu (hassas) olarak belirlenmesi, hassas konum belirleme ve uzay hava uygulamaları için önemli ve gereklidir.

İyonosferik gecikme Prezisyonlu Noktasal Konum Belirleme (Precise Point Positioning- PPP) uygulamalarında ana hata kaynaklarından biridir. TEC birinci derece iyonosferik gecikmeyi belirler. Çift frekanslı PPP kullanıcıları için, birinci derece iyonosferik gecikme, "iyonosfer içermeyen" (ionosphere-free) lineer kombinasyon olarak adlandırılan farklı frekanstaki iki sinyalin birleştirilmesi ile ortadan kaldırılabilir. Tek frekanslı PPP modeli için iyonosferik gecikme ek bir hata kaynağıdır. Modellenmemiş iyonosferik hata, konumlandırma doğruluğunu; özellikle yükseklik bileşeninde, düşürür. Bu nedenle, tek frekanslı PPP kullanıcılarının iyonosferik gecikme hesaplayabilmesi için bir düzeltme modeli kullanmaları gerekmektedir. Bu amaçla, gerçek zamanlı (Real Time) ve gözlem sonrası (Post Process) değerlendirme uygulamaları için birçok ampirik model, fiziksel model, bölgesel ve global iyonosferik harita geliştirilmiştir. Ancak, bu modeller sınırlı uzay-zamansal (spatiotemporal) çözünürlüklere sahip olduklarından tek frekanslı PPP uygulamaları için yeterli olmayabilmektedir.

Buna ek olarak, birçok iyonosferik gecikme düzeltme modeli literatürde bulunan önceki çalışmalarda önerilmiştir. Ancak, bu çalışmalar da verilen modeller bazı sınırlı mekânsal ve zamansal çözünürlüklere sahiptir. Bu nedenle, belirtilen sorunu aşmak için, bu çalışmada örnek bölge Avrupa seçilerek tek frekanslı PPP kullanıcıları için bölgesel ionosferik hata düzeltme modellerinin oluşturulması ele alınmaktadır.

Öncelikle Avrupa için Bölgesel İyonosfer Modeli (Regional Ionospheric Model-RIM) geliştirilmiştir. Önerilen model sırasıyla 1º × 1º ve 15 dakika mekânsal ve zamansal çözünürlüğe sahiptir. Bu kapsamda 60 IGS ve EUREF referans istasyonundan oluşan bölgesel ağa ait GNSS gözlemleri Dikey Toplam Elektron İçeriği (Vertical Total Electron Content- VTEC) değerleri üretmek amacıyla Bernese 5.2 yazılımı kullanılarak değerlendirmeler yapılmıştır. Yeni önerilen RIM'i test etmek için, farklı istasyonlar için tek frekanslı PPP doğruluğu ve yakınsama süresi (convergence time) hesaplanmış ve IGS Global İyonosfer Haritaları (IGS-Global Ionosphere Maps- IGS-GIM) ile üç farklı gün için karşılaştırılmıştır. Bu aşamada "İyonosfer içermeyen" çift frekanslı PPP çözümleri karşılaştırma amaçlı kullanımıştır. Elde edilen sonuçlar önerilen RIM'in IGS-GIM modeli ile karşılaştırıldığında yakınsama süresini hızlandırdığını, konum belirleme doğruluğununun yatay, düşey ve 3D bileşenlerini sırasıyla %20, %45 ve %45 düzeylerinde arttırdığını göstermektedir.

Buna ek olarak, Gerçek zamanlı Bölgesel İyonosfer Modeli (Real Time Regional Ionosphere Model- RT-RIM) IGS Gerçek Zamanlı Servisi (IGS Real Time Servis-IGS-RTS) hassas uydu yörünge ve saat ürünleri kullanılarak geliştirilmiştir. Önerilen modelin mekansal ve zamansal çözünürlüğü, sırasıyla, 1º × 1º ve 15 dakikadır. 60 IGS ve EUREF referans istasyonundan oluşan bölgesel ağa ait GPS gözlemleri gerçek zamanlı VTEC değerleri üretmek amacıyla Bernese 5.2 yazılımı kullanılarak değerlendirmiştir. Yeni önerilen RIM'i test etmek için, farklı istasyonlar için tek frekanslı PPP doğruluğu ve yakınsama süresi hesaplanarak IGS-GIM ile üç ardışık gün için karşılaştırılmıştır. Bu yolla, RT-RIM ile elde edilen PPP yakınsama süresi ve konum belirleme doğruluğu test edilmiş ve IGS-GIM modeli ile elde edilenlerle karşılaştırmıştır. Bu kapsamda "İyonosfer içermeyen" çift frekanslı PPP çözümleri karşılaştırma amaçlı kullanımıştır. Elde edilen sonuçlar önerilen RIM'in IGS-GIM modeli ile karşılaştırıldığında yakınsama süresini önemli ölçüde hızlandırdığını göstermektedir. Ayrıca, PPP doğruluğunun yatay, düşey ve 3D bileşenlerini IGS-GIM modeline kıyasla sırasıyla %40, %55, ve %40 düzeylerinde arttırdığı görülmektedir.

Prezisyonlu toplam elektron içeriğini modellemek amacıyla, hem uydu hem de alıcı için Diferansiyel Kod Sapması (Differential Code Bias -DCB) hesaba katılmalıdır. Diferansiyel Kod Sapması, iki farklı frekansda kod gecikmeleri farkıdır. Uydu DCB değerleri, bir gün boyunca stabildir ancak alıcı DCB değerleri uydununki kadar stabil değildir. GPS gözlemleri genellikle bölgesel ve global ölçeklerde TEC modellemesi için kullanılmaktadır. Son zamanlarda, çoklu-sistem GNSS TEC modelleme yaygın olarak kullanılmaktadır. Çoklu-sistem GNSS teknolojileri, diğer bir deyişle birden fazla uygu konum belirleme sisteminin birleşimi gözlenen uyduların ve izlenen sinyallerin sayısını artırır. Ayrıca, çalışılan bölge için iyonosfer modelinin doğruluğunu artırıran İyonosfer Delme Noktası (İonosphere Pierce Point-IPP) için daha iyi bir kapsama alanı sağlar. Çoklu-sistem GNSS içinde ek DCB parametrelerinin hesaplanması gerekmektedir.

Bu nedenle, Çoklu-sistem GNSS Alıcısı Diferansiyel Kod Sapması (Multi-constellation GNSS Receiver Diffrential Code Bias- MGR-DCB) hesaplama modeli geliştirilmiştir. Önerilen model iyonosfer düzeltmesi getirilmiş pseudorange farklarıyla GPS, Galileo ve Beidou sinyalleri için alıcı DCB'lerini hesaplamaktadır. Bu model, bölgesel iyonosferik model 'pseudorange' farklarından iyonosfer hatalarını kaldırmak için geliştirilmiştir. Önerilen modelin mekansal ve zamansal

çözünürlüğü, sırasıyla, 1º × 1º ve 15 dakikadır. Geliştirilen MGR-DCB modelini test etmek için, örnek üç IGS Çoklu-sistem GNSS Test (IGS-MGEX) istasyonları alıcı DCB'leri üç farklı gün için değerlendirimiştir. Sonrasında, hesaplanan DCB değerleri yayınlanan MGEX değerleri ile karşılaştırmıştır. Elde edilen sonuçlara göre, hesaplanan DCB'ler ve MGEX arasındaki uyuşumda ortalama fark ve Karesel Ortalama Hatasının (KOH) 1 ns den daha az olduğu görülmektedir. Ayrıca, GPS, Galileo ve Beidou gözlemlerinden hesaplanan VTEC değerleri IGS-GIM'den hesaplanan değerlerle karşılaştırılmıştır. Hesaplanan VTEC değerlerinin ortalama fark ve KOH değerlerinin 1 Toplam Elektron İçeriği Birimi (Total Electron Content Unit- TECU)'den daha az oldugu görülmektedir.

Elde edilen sonuçlara göre, konum belirleme doğruluğu CBS, hidrografik ölçmeler ve uzaktan algılama uygulamaları dahil bir çok uygulamada kullanılabilir olduğu sonucuna varılabilir. Buna ek olarak, gelişmiş MGR-DCB değerlendirmeleri prezisyonlu iyonosfer izleme ve uzay hava uygulamalarında da kullanılabilir.

1. INTRODUCTION

1.1 Background

The Earth's ionosphere is the layer from approximately 50 km up to 1000 km or more above the surface of the Earth. It consists of the ionized particles created by the Sun's Extreme Ultra Violation (EUV) and the X-ray radiations (Prolss, 2004). The collision of the energetic particles with the upper atmosphere is another source of ionization particularly at high latitudes (Kelley, 2009). Ionosphere essentially consists of four main layers, including the D-layer, the E-layer, the F1-layer and F2-layer, respectively (Hunsucker and Hargreaves, 2003). The electron density differs with the altitude, where its maximum value is at F2-layer (Schunk and Nagy, 2009).

The ionosphere is a region of freely charged electrons quantified by the total electron content, which is the total number of electrons along the line-of-sight between the satellite and the receiver. It is expressed in TEC unit (i.e., TECU= 10^{16} electron/m^2). The total electron content has a diurnal, a monthly, a seasonal and the so-called 11-year solar cycle variations. It also varies spatially, depending on the geographic location. The ionosphere activity depends on the solar and geomagnetic activities. The solar activity is the variation of the sun magnetic field, which can be expressed by two indices including the Sun Spot Number (SSN) and the solar flux index ($F_{10.7}$) (Memarzadeh, 2009). The geomagnetic activity is the natural variation of the geomagnetic field, where it can be expressed by two main indices including the planetary K_p-index and the planetary A_p-index (Hunsucker and Hargreaves, 2003).

The Earth's ionosphere is a dispersive medium, which means that the signal propagation velocity is frequency dependent. It speeds up the carrier phase observations beyond the speed of the light, whereas it delays the code observations. Moreover, it introduces the phase and amplitude scintillation (Hofmann-Wellenhof et al, 2008). The ionospheric delay ranges from less than 1 m to tens of metres during high ionospheric activities. Therefore, precise determination of the ionosphere total

electron content at both of global and regional scales is essential for precise positioning and space weather applications.

Precise point positioning technique is the processing of the un-differenced code and carrier phase observations from single receiver using the precise satellite orbit and clock products. It is firstly introduced by Zumberge et al. (1997). PPP provides centimeter- to decimeter-level positioning accuracy in static and kinematic modes. Precise point positioning is categorized into the dual-frequency PPP model and the single-frequency PPP model.

Traditionally, dual-frequency PPP model uses the un-differenced ionosphere-free linear combination of the code and carrier phase observations in order to remove the ionospheric error. The IGS precise orbit and clock products are used in order to account for the satellite orbit and clock errors, respectively. The tropospheric delay can be modeled using a proper model, including Hopfield or Saastamoinen model (Hofmann-Wellenhof et al, 2008). The effects of satellite and receiver antenna offsets, phase wind-up, relativistic errors, Sagnac effects, site displacement effects, solid earth tides and ocean loading, are accounted for using the models described in Kouba (2009).

For the single-frequency PPP model, the ionospheric delay is an additional error source. The un-modeled ionospheric error degrades the positioning accuracy, particularly the height component. Therefore, an ionospheric delay correction model must be used. For this purpose, a number of models have been developed for real-time and post processing applications, including empirical models, physical models, regional and global ionospheric maps. Unfortunately, however, those models have limited spatiotemporal resolution, which may not be adequate for single-frequency PPP applications.

For precise TEC modeling, the differential code bias for both of the satellites and the receiver must be accounted for. Differential code bias is the difference in the code hardware delays at two different frequencies. The satellite DCB values are stable over one day, while the receiver DCBs are not as stable (Schaer, 1999). Hardware delays are categorized as satellite hardware delay and receiver hardware delay. Satellite hardware delay is the time delay which is caused by the signal generation inside the satellite signal generator and the signal transmission by the satellite

antenna (El-Rabbany, 2006). Receiver hardware delay is occurred as the GNSS signal passes through the receiver antenna, analog hardware and digital processing to the point where pseudorange and carrier phase observations are physically made within the digital receiver channels (Kaplan and Hegarty, 2006).

GPS has traditionally been used for the development of regional and global ionospheric models. Recently, multi-constellation GNSSs have been used extensively in ionosphere modeling and monitoring applications. The fusion of multi-GNSS increases the number of the observed satellites and the tracked signals. Also, it provides better coverage of the Ionosphere Pierce Point (IPP), which enhances the accuracy of the ionospheric model for such studied area. Within the multi-constellation GNSS, additional DCB parameters must be estimated.

1.2 Previous Studies and Limitations

A number of ionospheric delay correction models have been developed by a number of researchers (e.g., Gao, 2007; Memarzadeh, 2009; Nohutcu, 2009; Durmaz, 2013; Liu et al., 2011; Ohashi et al., 2011; Zhang et al., 2013; Durmaz and Karslioglu, 2015; Li et al., 2015). Tu et al. (2013b) proposed a method for ionosphere total electron content modeling using simulated real-time data. The model was validated for three different networks on local, regional and global scales using the polynomial and spherical harmonic functions, respectively. The vertical total electron content and receiver DCB values were assessed and compared with the final IGS counterparts. The results showed that the estimated parameters were very consistent with the IGS counterparts. Moreover, the proposed model was validated for single-frequency PPP applications. It was found that the positioning was the same, while the convergence time was enhanced in comparison with the IGS-GIM counterparts.

Kao et al. (2014) developed a regional ionospheric model using the GPS observations. The vertical total electron content was modeled using the Multivariate Adaptive Regression Splines (MARS) function. Then, a least-squares algorithm was developed in order to estimate the VTEC and receiver DCB parameters for a 2-hour time interval. To validate their proposed model, the VTEC values were estimated and compared with the IGS-GIM counterparts. The estimated receiver DCB values were compared with the published IGS values. Moreover, the single-frequency PPP

obtained through the resulting VTEC were estimated and compared with those obtained through the IGS-GIM. The findings revealed that the estimated VTEC and receiver DCB values had good agreement with the IGS counterparts. In addition, the positioning accuracy using the proposed model was improved in comparison with the IGS-GIM.

The major limitation of the aforementioned models is that they had some limited spatial or temporal resolutions. In addition, the simulated real-time data mode does not represent the actual ionosphere characteristics in such area under consideration and the real-time single-frequency PPP deficiencies.

The estimation of the GPS differential code bias have been investigated by a number of studies (e.g., Arikan et al., 2008; Choi et al., 2011; Jin et al., 2012; Keshin, 2012; Kao et al., 2013). Keshin (2012) proposed a method for the receiver DCB estimation using the VETC values extracted from the IGS-GIM. The least-squares estimation algorithm has been used in order to determine the receiver DCB and vertical residual ionospheric delay. The estimated parameters have been compared with the IGS counterparts. The results showed agreement with the IGS values with differences less than 1ns.

More recently, the estimation of the multi-GNSS satellite and receiver differential code biases parameters have been investigated by a number of researchers (e.g., Montenbruck et al., 2014; Yinhua et al., 2014; Guo et al., 2015; Xue et al., 2015; Wang et al., 2015). Montenbruck et al. (2014) proposed a model for the multi-GNSS satellite and receiver DCBs estimation using the ionosphere-corrected pseudoranges differences. The IGS-GIM has been used to remove the ionospheric delay from the geometry-free linear combinations of the pseudorange observations. The DCBs for the legacy and modernized GPS, Galileo and BeiDou signals have been assessed and compared with the group delay parameters transmitted through the GNSS broadcast ephemeris data. It has shown that the estimated values had good agreement with the broadcast parameters.

The major drawback of the above mentioned DCB estimation models is that the IGS-GIM is used in order to remove the ionospheric error from the geometry-free linear combination of the code observations. The IGS-GIM, however, has a limited

spatiotemporal resolution which may not be adequate to represent the ionosphere variability in such studied area.

1.3 Study Objectives

The main objective of this study is to develop a high spatiotemporal resolution regional ionospheric model for single-frequency PPP users in Europe. The proposed model is developed in post processing and real-time domains. To validate the RIMs, the convergence time and the positioning accuracy obtained through the newly developed models are compared with those obtained through the IGS-GIM. Moreover, a multi-frequency multi-constellation GNSS receiver differential code bias model is proposed in order to precise modeling the ionosphere total electron content. A regional ionospheric model with spatial and temporal resolution of 1º×1º and 15 minutes, respectively, is developed to remove the ionospheric delay from the pseudorange differences. Then, the estimated receiver DCBs values are compared with the IGS-MGEX counterparts in order to validate the model.

1.4 Study Contributions

The contributions made in this study can be summarized as follows:

- Development of regional ionospheric model for single-frequency precise point positing users in Europe. The developed model has spatial and temporal resolution of 1º×1º and 15 minutes, respectively. The proposed model is validated for PPP applications in three different days to represent the ionospheric seasonal variations. The single-frequency PPP convergence time and positioning accuracy obtained through the proposed RIM are estimated and compared with those obtained through the IGS-GIM. The dual frequency ionosphere-free PPP is used as reference (Abdelazeem et al., 2016b).
- Development of real-time regional ionospheric model over Europe using the IGS-RTS precise satellite orbit and clock products. The newly proposed RT-RIM has spatial and temporal resolution of 1º×1º and 15 minutes, respectively. The single-frequency PPP convergence time and positioning accuracy obtained through the resulting RT-RIM using the RTS products are assessed and compared with those obtained through the rapid IGS-GIM in

three successive days under high solar activity, including one under active geomagnetic states. The dual frequency ionosphere-free PPP is used as reference (Abdelazeem et al., 2016a).

- Development of a multi-frequency multi-constellation GNSS receiver differential code bias estimation model. The newly proposed model estimates the receiver DCBs for GPS, BeiDou and Galileo signals. To validate the proposed model, the receiver DCB values for three stations from the IGS-MGEX are computed for three different days. The estimated DCBs values are compared with the publicly available IGS-MGEX counterparts. In addition, the combined GPS, BeiDou and Galileo VETCs are assessed and compared with the IGS-GIM counterparts (Abdelazeem et al., 2015).

1.5 Thesis Outline

The organization of the thesis depends basically on the following three Science Citation Index (SCI) and SCI Expanded journals publications as follows:

Chapter 1 consists of an introduction, previous studies and limitations, study objectives, study contributions and thesis outline.

Chapter 2 introduces the paper entitled with "An improved regional ionospheric model for single-frequency GNSS users".

Chapter 3 introduces the paper entitled with "An Enhanced Real-Time Regional Ionospheric Model Using IGS Real-Time Service (IGS-RTS) Products".

Chapter 4 introduces the paper entitled with "MGR-DCB: A Precise Model for Multi-constellation GNSS Receiver Differential Code Bias".

Chapter 5 introduces conclusion of this study and recommendations for the future works.

It should be pointed out that modifications to the original papers have been made only for proper identification of sections, figures and tables to assure uniformity within this thesis.

2. AN IMPROVED REGIONAL IONOSPHERIC MODEL FOR SINGLE-FREQUENCY GNSS USERS

2.1 Introduction

The Earth's ionosphere is the ionised portion of the upper layer of the atmosphere, which extends from approximately 50 km up to 1000 km or more above the surface of the Earth. It essentially consists of three layers: the D-layer, the E-layer and the F-layer, respectively. The Earth's ionosphere is a region of freely charged electrons quantified by the total electron content (TEC), which is the total number of electrons along the line-of-sight between the satellite and the receiver. TEC has a diurnal, a monthly, a seasonal and the so-called 11-year solar cycle variations. It also varies spatially, depending on the geographic location. The GNSS ionospheric delay ranges from less than 1 m to tens of metres during high ionospheric activities.

Mitigation of ionospheric delay is a major challenge for single-frequency precise point positioning (PPP) users. For this purpose, a number of models have been developed for real-time and post-processing applications, including the Klobuchar model, the IGS Global Ionospheric Maps (IGS-GIM) model and the NeQuick model (Klobuchar, 1987; Schaer, 1999; Nava et al., 2008). The coefficients of the Klobuchar model are transmitted to users as part of the GPS navigation message. Unfortunately, however, the Klobuchar model only corrects about 50% of the ionospheric delay. The NeQuick model was proposed for single-frequency Galileo users with performance superior to the Klobuchar model at different latitudes for the whole year (Oladipo and Schuler, 2012).

A widely used ionospheric mitigation method is the IGS-GIM product. A GIM file contains the vertical TEC (VTEC) values with a spatial resolution of 2.5° × 5° in latitude and longitude, respectively, and a temporal resolution of 2 hours.

This chapter is based on the paper: Abdelazeem, M., Çelik, R. N., & El-Rabbany, A. (2016b). An improved regional ionospheric model for single-frequency GNSS users. *Survey Review*, 1-7. doi:10.1080/00396265.2016.1138581.

Unfortunately, the IGS-GIM model has a limited spatiotemporal resolution, which may not be adequate for single-frequency PPP applications.

A number of regional ionospheric models (RIMs) have been proposed by a number of researchers (e.g., Bhuyan and Borah, 2007; Opperman et al., 2007; Alothman et al., 2011; Tu et al., 2013b; Yao et al., 2013; Abdelazeem et al., 2016a). Nohutcu et al. (2010) investigated the quadratic B-spline function to represent the VTEC using GPS observations over Turkey. Their results were comparable to those obtained through the Bernese software, which uses the spherical harmonic expansion. Durmaz et al. (2010) proposed a multivariate adaptive regression spline to represent the regional TEC using ground-based GPS observations over Europe. Their results showed similar root mean square error (RMSE) with those obtained through the Bernese software. However, the maps obtained through the Bernese software were rather smoother. Abdelazeem et al. (2016a) developed a real-time regional ionospheric model (RT-RIM) over Europe using the IGS real-time service (IGS-RTS) products. Their proposed model was validated for single-frequency PPP applications, where the positioning accuracy and convergence time obtained through the model were compared with those obtained through the IGS-GIM model. The results showed that the RT-RIM improved the PPP accuracy and convergence time by about 40, 55 and 40 % for the horizontal, height and 3D components, respectively, in comparison with the IGS-GIM.

This research aims to develop a RIM with a spatial and a temporal resolution of 1°×1° and 15 minutes, respectively, over Europe. The single-frequency PPP results obtained through the newly developed model are first compared with those obtained through the IGS-GIM model. In addition, the PPP positioning accuracy and convergence time are evaluated and compared with the dual-frequency ionosphere-free PPP counterpart. It is shown that the newly developed model improves the PPP accuracy and convergence time by about 20, 45 and 45 % for the 2D, height and 3D components, respectively, in comparison with the IGS-GIM model.

2.2 Ionospheric Model Development

The basic GPS observation equations can be expressed as follows (Kleusberg and Teunissen, 1998):

$$P_1 = \rho_r^s + c(dt_r - dt^s) + I_{r,1}^s + T_r^s + c\left(d_{r,1} + d_1^s\right) + \varepsilon_{p,1} \quad (2.1)$$

$$P_2 = \rho_r^s + c(dt_r - dt^s) + I_{r,2}^s + T_r^s + c\left(d_{r,2} + d_2^s\right) + \varepsilon_{p,2} \quad (2.2)$$

$$\varphi_1 = \rho_r^s + c(dt_r - dt^s) - I_{r,1}^s + T_r^s + c\left(\delta_{r,1} + \delta_1^s\right) + \lambda_1 N_1 + \varepsilon_{\varphi,1} \quad (2.3)$$

$$\varphi_2 = \rho_r^s + c(dt_r - dt^s) - I_{r,2}^s + T_r^s + c\left(\delta_{r,2} + \delta_2^s\right) + \lambda_2 N_2 + \varepsilon_{\varphi,2} \quad (2.4)$$

where P_1 and P_2 are the pseudorange measurements on L1 and L2, respectively; φ_1 and φ_2 are the carrier phase measurements on L1 and L2, respectively, in meter; ρ_r^s is the satellite-receiver true geometric range; c is the speed of light in vacuum; dt_r and dt^s are the receiver and satellite clock errors, respectively; $I_{r,1}^s$ and $I_{r,2}^s$ are the ionospheric delay on L1 and L2, respectively; T_r^s the tropospheric delay; d_r and d^s are the code hardware delay for the receiver and the satellite, respectively; δ_r and δ^s are the carrier phase hardware delay for the receiver and the satellite, respectively; λ_1 and λ_2 are the wavelength of the L1 and L2 carrier frequencies, respectively; N_1 and N_2 are the non-integer phase ambiguity parameters on L1 and L2, respectively; ε_p and ε_φ are the code and phase unmodeled errors, including noise and multipath.

The geometry-free linear combinations of code and carrier-phase observations are used to eliminate the geometrical term, tropospheric delay, receiver and satellite clock errors. It is obtained by subtracting the simultaneous un-differenced code or carrier-phase observations as follows (Dach et al., 2007):

$$P_4 = P_1 - P_2 = \left(1 - \frac{f_1^2}{f_2^2}\right) I_{r,1}^s + c(\Delta b^s + \Delta b_r) \quad (2.5)$$

$$\varphi_4 = \varphi_1 - \varphi_2 = \left(\frac{f_1^2}{f_2^2} - 1\right) I_{r,1}^s + c(\Delta\delta_r + \Delta\delta^s) + (\lambda_1 N_1 - \lambda_2 N_2) \quad (2.6)$$

where P_4 and φ_4 are the geometry-free linear combination for the code and carrier phase observations, respectively; Δb^s and Δb_r are the differential code bias (DCB)

for the satellite and the receiver, respectively; $\Delta\delta_r$ and $\Delta\delta^s$ are the differential phase hardware delay for the satellite and the receiver, respectively.

It is shown in Equations 2.5 and 2.6 that the geometry-free code linear combination contains the ionospheric delay and the DCBs of both of the receiver and the satellite. The geometry-free carrier-phase linear combination, on the other hand, contains the ionospheric delay, differential phase hardware delays of both of the receiver and the satellite and the ambiguity parameters. The slant TEC (STEC) along the satellite-receiver path can be estimated from the code or the carrier-phase observations. The carrier-phase observations are less noisy but biased by the ambiguity parameters. Therefore, the STEC is obtained from the carrier-smoothed code observations based on Equation 2.5 as follows:

$$STEC = \left(\frac{f_1^2 f_2^2}{40.3(f_2^2 - f_1^2)}\right)[P_4 - c\,(\Delta b^S + \Delta b_r)] \tag{2.7}$$

The STEC can be converted into VTEC by using the modified single layer model (MSLM) mapping function, which assumes that all free electrons are concentrated in a shell of infinitesimal thickness at a height H (Figure 2.1). This height (H) corresponds to maximum electron density at the F2 peak, which ranges from 350 km to 450 km. Therefore, the VTEC can be calculated at the point of intersection between the thin shell and the satellite-receiver path, known as ionosphere pierce point (IPP) (Schaer, 1999):

$$VTEC = STEC * cos\left(arcsin\left(\frac{R}{R+H}sin(\alpha z)\right)\right) \tag{2.8}$$

where z is the satellite's zenith distances at receiver, respectively (Figure 2.1); R is the mean radius of the Earth, and α is a correction factor. Best fit of the MSLM with respect to the JPL extended slab model (ESM) mapping function is achieved at $H = 506.76\,km$ and $\alpha = 0.9782$, when using $R = 6371\,km$ and assuming a maximum zenith distance of 80 degrees (Dach et al., 2007).

The VTEC can be modelled on a regional scale as a function $E(\beta, s)$ of the geographic latitude (β) and the sun-fixed longitude (s) of the IPP, respectively. The

regional VTEC is expressed as a spherical harmonic expansion, which takes the form (Dach et al., 2007):

$$E(\beta, s) = \sum_{n=0}^{n_{max}} \sum_{m=0}^{n} P_{nm}^{-}(sin\,\beta)\,(a_{nm}\,cos\,ms + b_{nm}\,sin\,ms) \tag{2.9}$$

where n_{max} is the maximum degree of the spherical harmonic expansion; P_{nm}^{-} are normalized associated Legendre functions of degree *n* and order *m*; a_{nm} and b_{nm} are the unknown spherical harmonics coefficients.

Substituting Equations 2.7 and 2.8 into Equation 2.9, the ionospheric spherical harmonic model can be expressed as:

$$\begin{aligned} &\sum_{n=0}^{n_{max}} \sum_{m=0}^{n} P_{nm}^{-}(sin\,\beta)\,(a_{nm}\,cos\,ms + b_{nm}\,sin\,ms) \\ &\quad = \left(\frac{f_1^2 f_2^2}{40.3(f_2^2 - f_1^2)}\right)[P_4 - c\,(\Delta b^S + \Delta b_r)] \\ &\quad * \; cos\left(arcsin\left(\frac{R}{R+H} sin(\alpha z)\right)\right) \end{aligned} \tag{2.10}$$

where a_{nm}, b_{nm}, Δb^S and Δb_r are the unknowns parameters to be computed.

In order to separate the DCBs of the satellites and receivers, an additional constraint must be used. It assumes that the sum of satellite DCBs is zero as follows (Dach et al., 2007):

$$\sum_{s=1}^{s=max} \Delta b^s = 0 \tag{2.11}$$

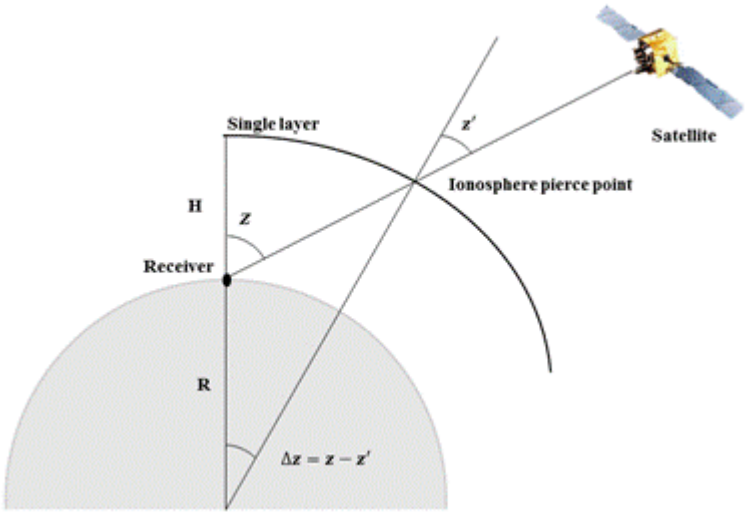

Figure 2.1 : Single layer model (SLM).

2.3 Methodology

A regional network consisting of 60 IGS and EUREF reference stations in Europe has been used to develop the proposed regional ionospheric correction model (Figure 2.2). The stations are homogeneously distributed in different latitudes in order to reflect different ionospheric characteristics. GNSS observations for three different days (day 150, 220 and 360 in year 2013) have been downloaded (IGS, 2015) to represent the ionosphere seasonal variations in May, August and December, respectively. Each observation file has a 24-hour time span and a 30-second time interval. An elevation cut-off angle of 20° has been used. The files have been processed using the Bernese software package in PPP mode. In order to produce the RIM, the IGS final satellite orbit, satellite clock and earth orientation parameters have been used (IGS, 2015) and then have been converted into the Bernese formats. The un-differenced code observations have been smoothed. In the parameters estimation process, the effective height has been selected to be 450 km. In addition, a maximum degree and order equal to six of the spherical harmonic expansion have been selected with a 15-minute interval. A group of 49 coefficients of the spherical harmonic model has been obtained each time epoch. Thereafter, to extract the VTEC maps a spatial and temporal resolution of 1° × 1° and 15 minutes, respectively, have been selected.

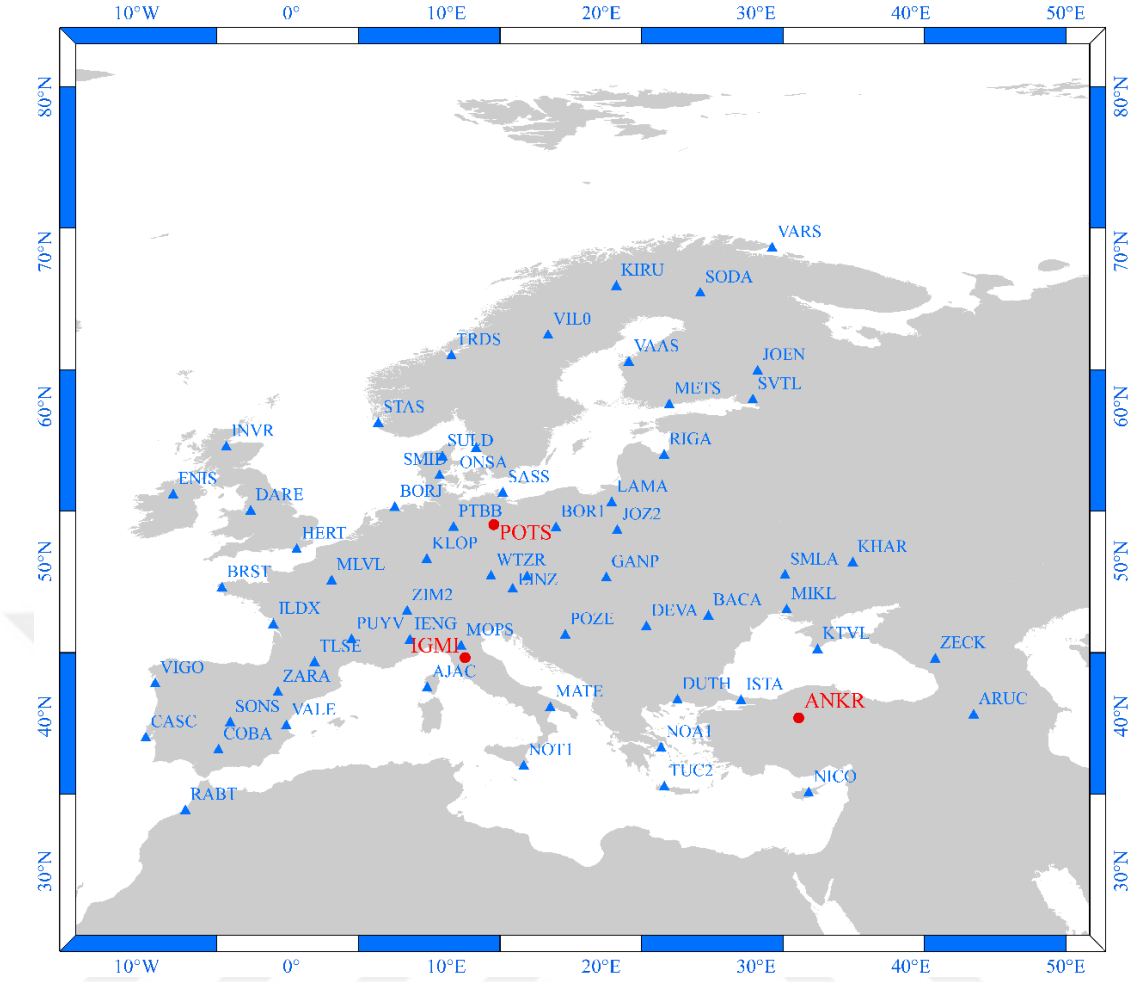

Figure 2.2 : Reference stations distribution (with triangle shape) and examined stations (with circular shape).

2.4 Results and Analysis

In order to evaluate the RIM, GNSS observations from another set of stations (Figure 2.2) have been processed using Natural Resources Canada (NRCan) GPSPace PPP software. The examined stations have been selected to represent different latitudes (Table 2.1). The IGS final precise orbit and clock products have been used to account for the satellite orbit and clock errors, respectively. The tropospheric delay has been accounted for using the Hopfield model with the Neil mapping function. The PPP accuracy and convergence times have been calculated and compared with those of the un-differenced dual-frequency ionosphere-free PPP and the single-frequency PPP obtained through the IGS-GIM model.

Table 2.1 : Examined stations characteristics.

Station	Latitude	Longitude	Receiver type
ANKR	39.8874°	32.7584°	TPS E_GGD
IGMI	43.7833°	11.2119°	TPS ODYSSEY_E
POTS	52.3793°	13.0661°	JAVAD TRE_G3TH DELTA

Figure 2.3 illustrates the convergence times for station POTS, IGMI and ANKR for DOY 150, 220 and 360, respectively, as examples. It can be seen that the use of RIM speeds up the convergence time in comparison with the IGS-GIM model.

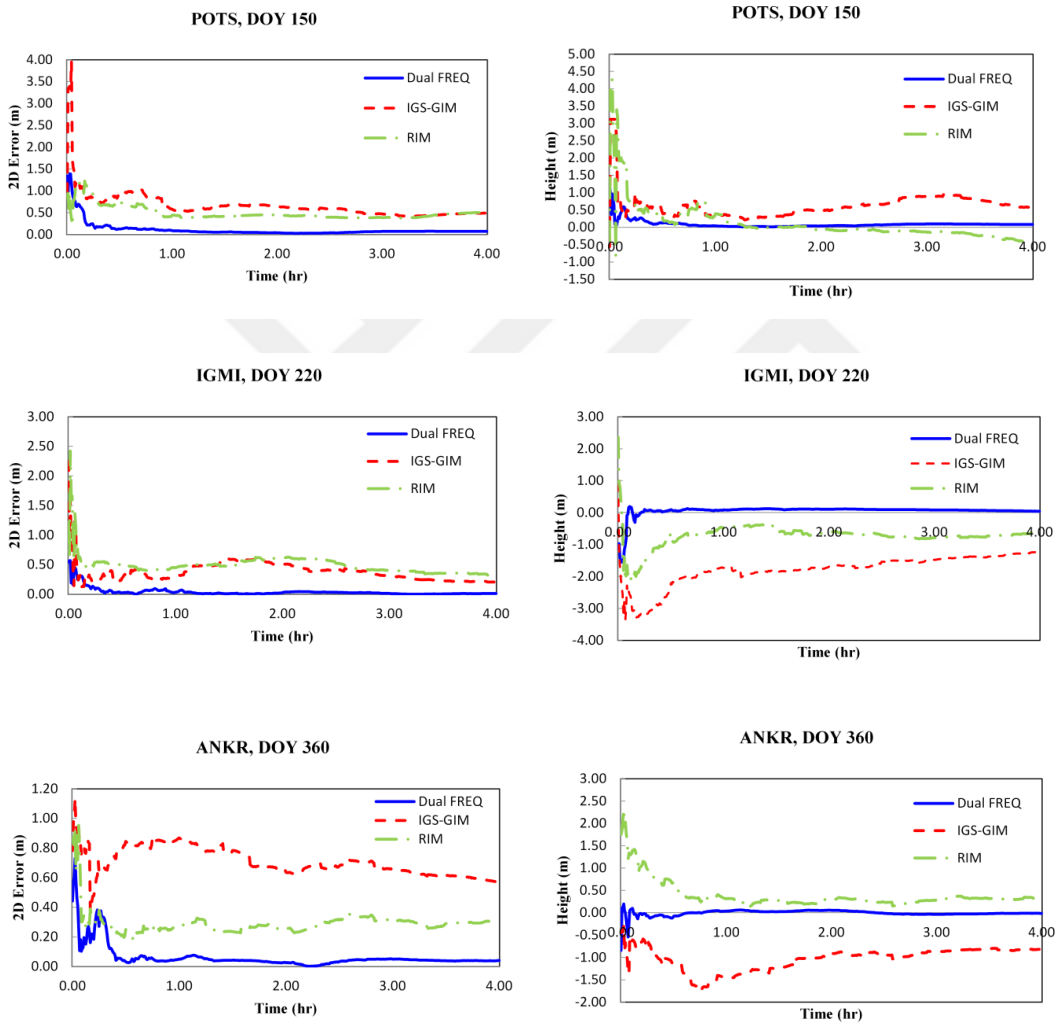

Figure 2.3 : Horizontal and height convergence time**.**

The estimated PPP station coordinates were compared with those of the EUREF final weekly counterparts and the standard deviations (STD) of the solutions were calculated. Table 2.2 summarises the mean difference and STD for the horizontal, height and 3D components for the three examined stations.

Table 2.2 : Positioning accuracy statistics.

Station	Statistical Analysis (m)	Ionosphere-free Dual Frequency			IGS-GIM			RIM		
		2D	H	3D	2D	H	3D	2D	H	3D
DOY 150										
ANKR	Mean	0.065	0.059	0.088	0.115	-0.844	0.852	0.198	0.592	0.624
	STD	0.013	0.024	0.027	0.193	0.328	0.380	0.188	0.315	0.367
IGMI	Mean	0.087	0.084	0.121	0.565	0.119	0.578	0.216	-0.212	0.303
	STD	0.018	0.025	0.031	0.192	0.388	0.433	0.187	0.390	0.433
POTS	Mean	0.072	0.082	0.109	0.488	0.580	0.758	0.507	-0.412	0.653
	STD	0.014	0.025	0.029	0.230	0.357	0.425	0.235	0.352	0.423
DOY 220										
ANKR	Mean	0.011	0.035	0.037	0.612	-1.090	1.250	0.562	0.373	0.675
	STD	0.020	0.030	0.036	0.161	0.299	0.339	0.160	0.270	0.314
IGMI	Mean	0.015	0.042	0.045	0.222	-1.262	1.281	0.327	-0.617	0.699
	STD	0.021	0.022	0.030	0.154	0.234	0.280	0.152	0.247	0.290
POTS	Mean	0.010	0.027	0.029	0.049	-0.764	0.766	0.237	-0.716	0.754
	STD	0.021	0.024	0.032	0.195	0.330	0.383	0.194	0.325	0.379
DOY 360										
ANKR	Mean	0.040	-0.014	0.042	0.565	-0.812	0.989	0.302	0.297	0.423
	STD	0.023	0.028	0.036	0.161	0.239	0.288	0.166	0.265	0.313
IGMI	Mean	0.071	-0.035	0.080	0.666	-0.920	1.136	0.396	0.282	0.486
	STD	0.021	0.030	0.036	0.228	0.401	0.461	0.201	0.410	0.457
POTS	Mean	0.052	0.005	0.053	0.347	-0.711	0.791	0.187	0.270	0.328
	STD	0.021	0.031	0.037	0.232	0.321	0.396	0.250	0.267	0.366

Based on the results presented in Table 2.2, it can be seen that the PPP positioning accuracy is improved when the RIM is used, in comparison with those of the IGS-GIM model. This is particularly signified in the height component. For station ANKR, the 2D positioning accuracy is improved when the RIM is used from 0.612 to 0.562 m and from 0.562 to 0.302 m on DOY 220 and 360, respectively. The error in the height component is also reduced from −0.844 to 0.592 m, from −1.09 to 0.373 m and from −0.812 to 0.297 m on DOY 150, 220 and 360, respectively. For station IGMI, the horizontal positioning accuracy of the RIM is also found superior to that of the IGS-GIM where it is changed from 0.565 to 0.216 m and from 0.666 to 0.396 m on DOY 150 and 360, respectively. An exception is the results on DOY 220. For the height component, its accuracy is improved from −1.262 to −0.617 m and from −0.92 to 0.282 m on DOY 220 and 360, respectively. No improvement in the height component was obtained on DOY 150. For station POTS, the 2D positioning accuracy is improved from 0.347 to 0.187 m on DOY 360. Approximately the same value was obtained from both models on DOY 150. The accuracy of the height component is significantly improved from 0.58 to −0.412 m, from −0.764 to −0.714 m and from −0.711 to 0.27 m over the three days under consideration.

Figure 2.4 shows the statistical results for the 2D and 3D PPP accuracy obtained through the RIM, in comparison with those of the un-differenced ionosphere-free dual frequency and IGS-GIM models for the three examined stations on DOY 150, 220 and 360, respectively. It can be seen that the obtained 3D positioning accuracy is significantly improved with the RIM is used, in comparison with the IGS-GIM model. As an example, the 3D error for station ANKR is reduced from 0.852 to 0.624 m, from 1.250 to 0.675 m and from 0.989 to 0.423 m on DOY 150, 220 and 360, respectively. For station IGMI, the 3D positioning accuracy is improved from 0.578 to 0.303 m, from 1.281 to 0.699 m and from 1.136 to 0.486 m in the three examined days, respectively. Finally, the 3D positioning accuracy for station POTS is improved from 0.758 to 0.653 m, from 0.766 to 0.754 m and from 0.791 to 0.328 m on DOY 150, 220 and 360, respectively.

Table 2.3 summarises the statistical parameters, including the mean, maximum, minimum and RMSEs values for the positioning accuracy of the single-frequency PPP obtained through the IGS-GIM and the RIM, with respect to the ionosphere-free dual frequency solution. It can be said that the overall positioning accuracy is improved by about 20, 45 and 45 % in horizontal, height and 3D components, respectively, in comparison to the IGS-GIM model.

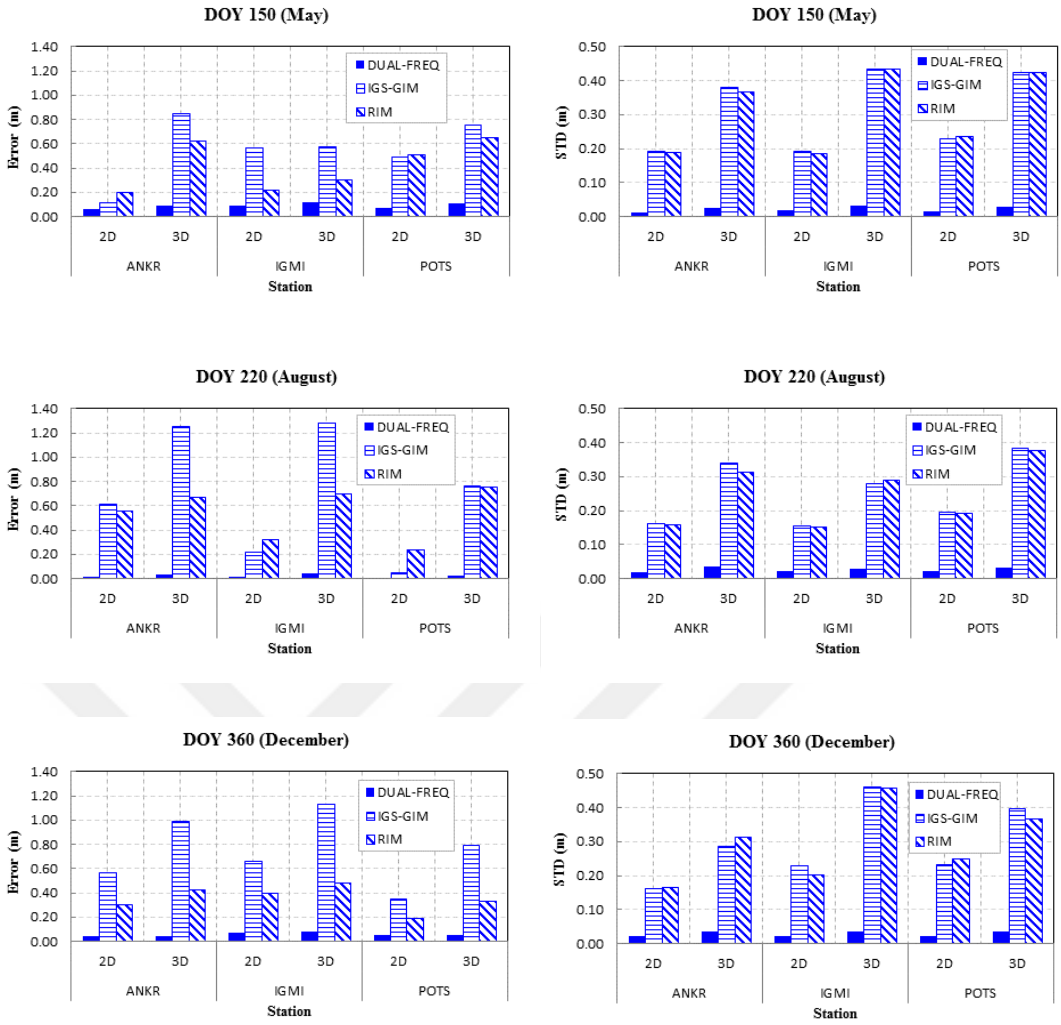

Figure 2.4 : 2D and 3D statistical results**.**

Table 2.3 : Statistical parameters for the positioning accuracy results.

Statistical parameter (m)	IGS-GIM			RIM		
	2D	H	3D	2D	H	3D
Mean	0.356	0.784	0.866	0.279	0.440	0.482
Min.	0.039	0.035	0.457	0.129	0.265	0.182
Max.	0.601	1.304	1.236	0.551	0.743	0.725
RMSE	0.207	0.538	0.249	0.137	0.467	0.173

2.5 Conclusion

In this paper, a RIM with a 1° × 1° spatial resolution and a 15-minute temporal resolution has been developed. GNSS observations from 60 IGS and EUREF reference stations over Europe have been processed using the Bernese software package to develop the model. In order to validate the developed model, the PPP convergence time and positioning accuracy for another set of stations in three different days have been estimated and compared with those of the IGS-GIM and ionosphere-free dual frequency counterparts. The results reveal that the proposed model speeds up the convergence time. In addition, the overall positioning accuracy has improved in comparison with the IGS-GIM counterpart by about 20, 45 and 45 % for the 2D, height and 3D components, respectively.

3. AN ENHANCED REAL-TIME REGIONAL IONOSPHERIC MODEL USING IGS REAL-TIME SERVICE (IGS-RTS) PRODUCTS

3.1 Introduction

The estimation of the ionosphere Total Electron Content (TEC) and its change is an important issue for precise positioning and space weather applications. Ionospheric delay is the dominant error source in single frequency Precise Point Positioning (PPP). Therefore, mitigation of ionospheric delay in real-time is a major challenge for single-frequency PPP users.

In order to provide real-time PPP users with more precise products, the International Global Navigation Satellite System (GNSS) Service (IGS) has launched its Real-Time Service (IGS-RTS). The RTS has become available through the collaboration of Natural Resources Canada (NRCan), the German Federal Agency for Cartography and Geodesy (BKG), and the European Space Agency's Space Operations Centre in Darmstadt, Germany (ESA/ESOC) with the support of 160 stations, multiple data centres, and ten analysis centres around the world. The service has been available since 1 April 2013 (Hadas and Bosy, 2015).

The RTS analysis centres compute the GNSS clock corrections to the broadcast ephemeris using IGS ultra-rapid predicted orbits and real-time data streams from the real-time reference stations. The real-time solutions of each analysis centre are combined into a real-time correction product and then sent to users. Currently, the available RTS products include GPS-only correction streams. IGS01/IGC01 is a single-epoch combination solution. IGS02 is a Kalman filter combination solution. IGS03 is a Kalman filter GPS and GLONASS combination correction provided as an experimental product. In addition, RTS provides two streams of real-time broadcast ephemeris; RTCM3EPH01 for GPS orbits and RTCM3EPH for GPS, GLONASS

This chapter is based on the paper: Abdelazeem, M., Çelik, R. N., & El-Rabbany, A. (2016a). An Enhanced Real-Time Regional Ionospheric Model Using IGS Real-Time Service (IGS-RTS) Products. *Journal of Navigation, 69(3),* 521-530.

and Galileo. More details on RTS products and their quality assessment can be found in Caissy et al. (2012) and Hadas and Bosy (2015).

The accuracy of Real-Time Precise Point Positioning (RT-PPP) using the RTS products have been investigated by a number of researchers (e.g., Chen at al., 2010; Rovira-Garcia et al., 2012; Chen et al., 2013 and Li et al., 2014). Chen et al. (2010) investigated the accuracy of IGS-RT products in kinematic PPP mode. The results showed that the achieved position precision was about ± 2–4 cm and 6–8 cm in horizontal and height components, respectively. Chen et al. (2013) evaluated the accuracy of real-time products in static and kinematic real-time PPP for 41 IGS reference stations. The results revealed that the accuracy of static PPP was of ± 2-3 cm in the North and ± 3–4 cm in the other components, while for the kinematic PPP the obtained accuracy was ± 2.2 cm, 4.2 cm, and 6.1 cm in the north, east, and up directions, respectively.

The objective of this paper is to develop a Real-Time Regional Ionospheric Model (RT-RIM) over Europe using the RTS satellite orbit and clock products. GPS observations from 60 IGS and EUREF reference stations are processed using the Bernese 5.2 PPP module in order to produce Real-Time Vertical Electron Content (RT-VTEC) with a spatial and temporal resolution of 1° × 1° and 15 minutes, respectively. The single-frequency PPP obtained through the developed model is compared with those obtained through the combined rapid IGS-GIM. The PPP positioning accuracy and convergence time are also computed and compared with the dual-frequency ionosphere-free PPP counterparts.

It shown that the proposed model improves the PPP accuracy and convergence time about 40%, 55% and 40% for the horizontal, height and 3D components, respectively in comparison with the IGS-GIM.

3.2 Proposed Real-Time Ionospheric Model

The basic GPS observation equations can be expressed as follows (Kleusberg and Teunissen, 1998):

$$P_i = \rho_r^s + c(dt_r - dt^s) + I_{r,i}^s + T_r^s + c\left(d_{r,i} + d_i^s\right) + \varepsilon_{p,i} \quad (3.1)$$

$$\varphi_i = \rho_r^s + c(dt_r - dt^s) - I_{r,i}^s + T_r^s + c\left(\delta_{r,i} + \delta_i^s\right) + \lambda_i N_i + \varepsilon_{\varphi,i} \quad (3.2)$$

where P_i and φ_i are the pseudorange and carrier phase measurements in meter, respectively; ρ_r^s is the satellite-receiver true geometric range; c is the speed of light in vacuum; dt_r and dt^s are the receiver and satellite clock errors, respectively; $I_{r,i}^s$ the ionospheric delay; T_r^s the tropospheric delay; $d_{r,i}$ and d_i^s are the code hardware delay for the receiver and the satellite, respectively; $\delta_{r,i}$ and δ_i^s are the carrier phase hardware delay for the receiver and the satellite, respectively; λ_i is the wavelength of carrier phase; N_i is the non-integer phase ambiguity, and $\varepsilon_{p,i}$ and $\varepsilon_{\varphi,i}$ are the code and phase unmodeled errors, including noise and multipath.

Geometry-free linear combinations are formed using the un-differenced carrier smoothed code observations, which eliminate the geometrical term, tropospheric delay, receiver and satellite clock errors as follows (Dach et al., 2007):

$$P_4 = P_1^- - P_2^- = \left(1 - \frac{f_1^2}{f_2^2}\right) I_r^s + c(\Delta b^s + \Delta b_r) \quad (3.3)$$

where P_i^- is the smoothed code observables; I_r^s is the L1 ionospheric delay; c is the light speed in vacuum; Δb^s and Δb_r are the Differential Code Bias (DCB) for the satellite and the receiver, respectively.

The DCB is the difference in the code hardware delays at two different frequencies. The slant TEC along the satellite-receiver path can be determined based on Equation (3.3) as follows:

$$STEC = \left(\frac{f_1^2 f_2^2}{40.3(f_1^2 - f_2^2)}\right)[P_4 + c\,(\Delta b^S + \Delta b_r)] \quad (3.4)$$

The vertical TEC can be determined using the Modified Single Layer Model (MSLM) mapping function that assumes that all free electrons are concentrated in a shell of infinitesimal thickness at height H. The effective height (H) corresponds to maximum electron density at the F2 peak ranges from 350 km to 450 km. The VTEC is determined at the Ionosphere Pierce Point (IPP), the point of intersection between the shell layer and satellite-receiver path, as given below (Schaer, 1999):

$$VTEC = STEC * cos\left(arcsin\left(\frac{R}{R+H} sin(\alpha z)\right)\right) \quad (3.5)$$

where z is the satellite's zenith distance at the receiver; R is the mean radius of the Earth, and α is a correction factor. Best fit of the MSLM with respect to the JPL Extended Slab Model (ESM) mapping function is achieved at $H = 506.76\,km$ and $\alpha = 0.9782$, when using $R = 6371\,km$ and assuming a maximum zenith distance of 80° (Dach et al., 2007).

The VTEC can be modeled on a regional scale as a function E(β, s) of the geographic latitude (β) and the sun-fixed (s) longitude of the IPP, respectively. The regional VTEC is expressed as a spherical harmonic expansion, which takes the form (Schaer, 1999):

$$E(\beta, s) = \sum_{n=0}^{n_{max}} \sum_{m=0}^{n} P_{nm}^{-}(sin\,\beta)\,(a_{nm}\,cos\,ms + b_{nm}\,sin\,ms) \quad (3.6)$$

where n_{max} is the maximum degree of the spherical harmonic expansion; P_{nm}^{-} are normalized associated Legendre functions of degree *n* and order *m*; a_{nm} and b_{nm} are the unknown coefficients of spherical harmonics.

Substituting Equations (3.4) and (3.5) into Equation (3.6), the ionospheric spherical harmonic model can be expressed as:

$$\sum_{n=0}^{n_{max}} \sum_{m=0}^{n} P_{nm}^{-}(sin\,\beta)\,(a_{nm}\,cos\,ms + b_{nm}\,sin\,ms) = \left(\frac{f_1^2 f_2^2}{40.3(f_1^2 - f_2^2)}\right)[P_4 + c\,(\Delta b^S + \Delta b_r)] * cos\left(arcsin\left(\frac{R}{R+H} sin(\alpha z)\right)\right) \quad (3.7)$$

where a_{nm}, b_{nm}, Δb^S and Δb_r are the unknowns parameters to be computed.

In order to separate the DCBs of the satellites and receivers, an additional constraint must be used. It assumes that the sum of satellite DCBs is zero (Equation 3.8).

$$\sum_{s=1}^{s=max} \Delta b^s = 0 \tag{3.8}$$

3.3 Methodology

A regional network consisting of 60 IGS and EUREF reference stations in Europe has been used to develop the Real-Time Regional Ionospheric Model (RT-RIM) (Figure 3.1). The station distribution represents different latitudes in order to reflect different ionospheric characteristics. GPS observations for three successive days (Day Of Year (DOY) 30, 31 and 32 in 2015) have been downloaded (BKG, 2015). Table 3.1 shows the radio flux at 10.7 cm wavelength (F10.7) index (NICT-SWIC, 2015) and geomagnetic planetary (AP) index (GFZ, 2015) in the three days that represent the solar and geomagnetic activity, respectively. As shown in Table 3.1, the solar activity is high in the three days, while the geomagnetic activity is unsettled in the first two days and active in the third day.

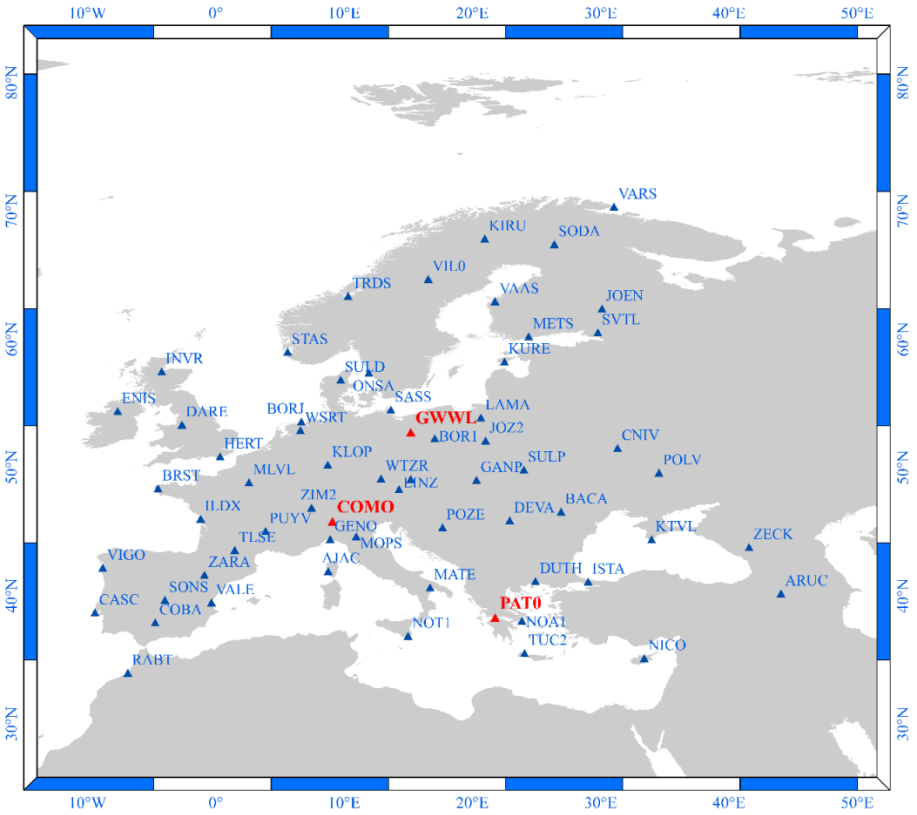

Figure 3.1 : Stations distribution.

Table 3.1 : $F_{10.7}$ and A_P indices for the examined days (NICT-SWIC, 2015; GFZ, 2015).

DOY	Solar Flux-$F_{10.7\ cm}$	Geomagnetic index- A_P
30	159	9
31	154	9
32	142	20

Each observation file has a 24-hour time span and a 30-second time interval. The observation files have been processed using the Bernese 5.2 software package using the PPP module. In order to produce the RT-RIM, the IGS-RTS satellite orbit and clock products (IGS-RTPP, 2015) have been used and then have been converted into the Bernese formats. The un-differenced code observations have been smoothed. In the parameters estimation process, the effective height has been selected to be 450 km. In addition, a maximum degree and order equal to six of the spherical harmonic expansion has been selected with a 15-minute interval. A group of 49 coefficients of the spherical harmonic model has been obtained for each time epoch. Thereafter, to extract the VTEC maps a spatial and temporal resolution of 1° × 1° and 15 minutes, respectively, have been selected. Figure 3.2 shows the flow chart of the proposed steps for the RT-RIM and its evaluation procedure.

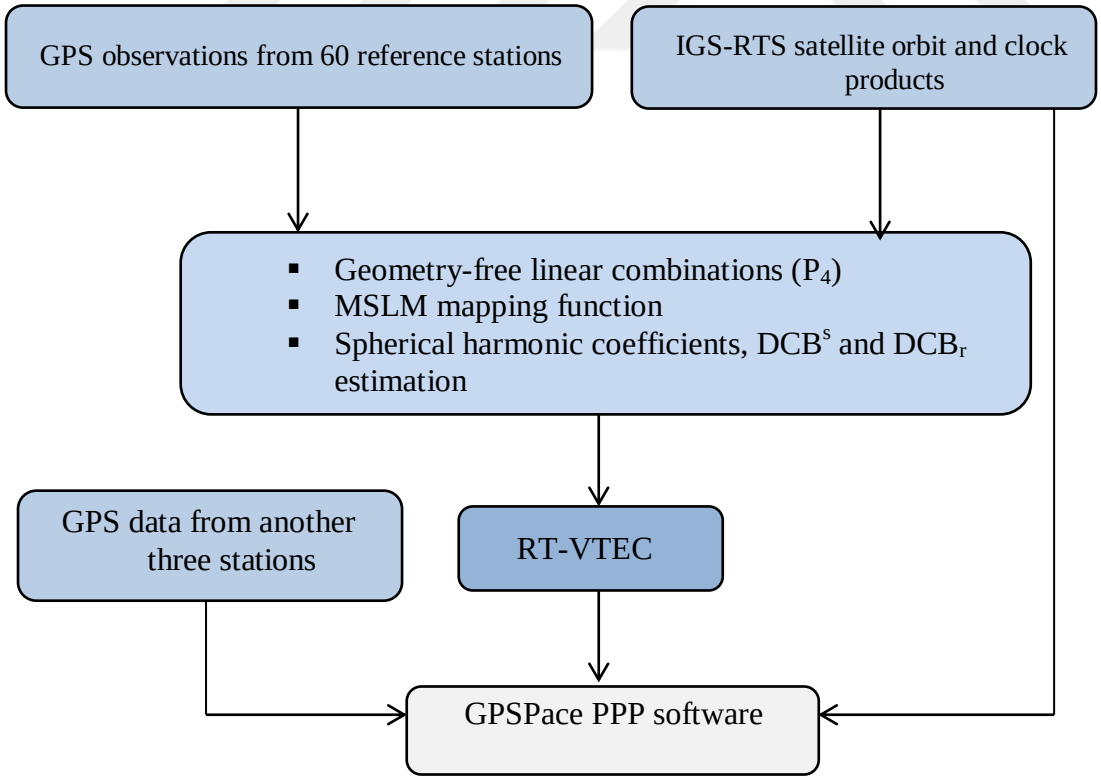

Figure 3.2 : Flow chart of the proposed RT-RIM.

3.4 Results and Analysis

In order to evaluate the developed RT-RIM, GPS observations from another set of stations (Figure 3.1 in red) were processed using Natural Resources Canada (NRCan) GPSPace PPP software. The GPS observation time window was six hours starting from 12 UT. The tested stations were selected to represent different latitudes (Table 3.2). The IGS–RTS precise orbit and clock products were used to account for the satellite orbit and clock errors, respectively. For the modernised C1/P2 receivers, the data was corrected using the P1-C1 DCBs in order to be consistent with the satellite clock corrections convention. In addition, the tropospheric delay was modelled using the Hopfield model with the Neil mapping function. The PPP positioning accuracy was calculated and compared with the un-differenced dual frequency ionosphere-free and single-frequency using the combined rapid IGS-GIM model. For the PPP positioning processes of the dual frequency ionosphere-free and the IGS-GIM model, the rapid IGS precise satellite orbit and clock products (IGS, 2015) were used to remove the satellite orbit and clock errors.

Table 3.2 : Tested stations characteristics.

Station	Latitude	Longitude	Receiver type	Antenna type
PAT0	38.2837	21.7868	TPS NET-G3A	ASH700936E-NONE
COMO	45.8022	9.0956	TPS E_GGD	TPSCR3_GGD-CONE
GWWL	52.7380	15.2052	TRIMBLE NETR9	TRM59900.00-SCIS

Similar convergence times are obtained for each station in the three days. For illustration purposes, only the convergence times for station GWWL, PAT0 and COMO on DOY 30, 31 and 32, respectively are shown in Figure 3.3 as examples. It is seen that the RT-RIM accelerates the convergence time with respect to the IGS-GIM model.

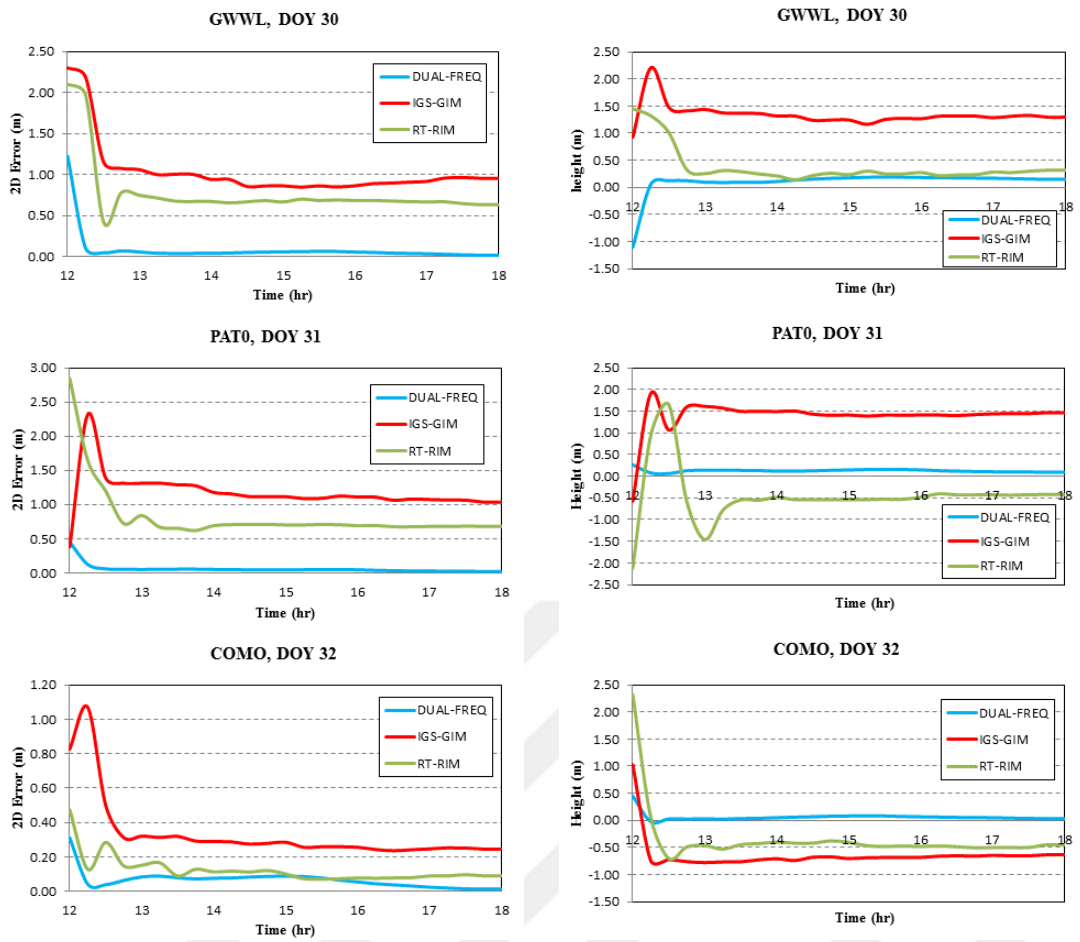

Figure 3.3 : PPP convergence time.

The computed PPP station coordinates were compared with those of the EUREF final weekly counterparts. Table 3.3 summarises the mean difference for the horizontal, height and 3D components for the three examined stations.

Table 3.3 : Positioning accuracy differences.

DOY	Station	Ionosphere-free Dual Frequency			IGS-GIM			RT-RIM		
		2D	H	3D	2D	H	3D	2D	H	3D
30	PAT0	0.037	0.093	0.100	0.883	1.329	1.595	0.415	0.645	0.767
	COMO	0.040	0.006	0.041	0.644	-0.485	0.806	0.352	0.792	0.867
	GWWL	0.018	0.147	0.148	0.956	1.296	1.610	0.634	0.317	0.709
31	PAT0	0.022	0.094	0.097	1.036	1.467	1.796	0.682	-0.421	0.802
	COMO	0.033	0.013	0.035	0.137	-0.574	0.590	0.241	0.375	0.446
	GWWL	0.021	0.147	0.148	0.929	0.260	0.964	0.698	-0.321	0.768
32	PAT0	0.034	0.089	0.095	0.947	0.212	0.971	0.957	-0.529	1.094
	COMO	0.013	0.031	0.034	0.246	-0.634	0.680	0.091	-0.450	0.459
	GWWL	0.029	0.132	0.135	1.068	-1.161	1.578	0.577	-0.170	0.602

As given in Table 3.3, the PPP positioning accuracy is improved when the RT-RIM is used, in comparison with IGS-GIM model. For station PAT0, the 2D positioning accuracy obtained from the RT-RIM is improved from 0.833 m to 0.415 m and from 1.036 m to 0.682 m on DOY 30 and 31, respectively. The accuracy of the height component is also improved from 1.329 to 0.645 m and from 1.467 m to 0.421 m on DOY 30 and 31, respectively. An exception is the results on DOY 32. For station COMO, the RT-RIM horizontal positioning accuracy is better than that of the IGS-GIM, where it is changed from 0.644 m to 0.352 m and from 0.246 m to 0.091 m in DOY 30 and 32, respectively. An exception is the results on DOY 31. The error in the height component is reduced from 0.574 m to 0.375 m and from 0.634 m to 0.450 m in DOY 31 and 32, respectively. An exception is the results on DOY 30. For station GWWL, the 2D positioning accuracy of the RT-RIM is also superior to that of the IGS-GIM model, where it is improved from 0.956 m to 0.634 m, from 0.929m to 0.698 m and from 1.068 m to 0.577 m on DOY 30, 31 and 32, respectively. In addition, the error in the height component is reduced from 1.296 m to 0.317 m and from 1.161 m to 0.17 m on DOY 30 and 32, respectively. An exception is the results on DOY 31.

Figure 3.4 shows the horizontal and 3D PPP accuracy obtained through the RIM, in comparison with those of the un-differenced ionosphere-free dual frequency and IGS-GIM models for the three examined stations on DOY 30, 31 and 32, respectively. It can be seen that the obtained 3D positioning accuracy is improved when the RIM is used, in comparison with the IGS-GIM model. For instance, the 3D accuracy for station PAT0 is improved from 1.595 m to 0.767 m and from 1.796 m to 0.802 m on DOY 30 and 31, respectively. For station COMO, the 3D error is decreased from 0.590 m to 0.446 m and from 0.680 m to 0.459 m on DOY 31 and 32, respectively. The 3D positioning accuracy is also improved for station GWWL, where it is reduced from 1.610 m to 0.709 m, from 0.964 m to 0.768 m and from 1.578 m to 0.602 m on DOY 30, 31 and 32, respectively.

It is seen that in three cases the positioning accuracy obtained from the IGS-GIM model is slightly better than the RT-RIM, this is because the ionospheric delay value extracted from the IGS-GIM is more accurate than the one extracted from the RT-RIM, where the IGS-GIM is a combination of four analysis centres with different ionosphere modelling methods.

Based on the previous results, it can be concluded that the RT-RIM typically improved the positioning accuracy and convergence time by about 40%, 55% and 40% for the horizontal, height and 3D components respectively in comparison with the IGS-GIM.

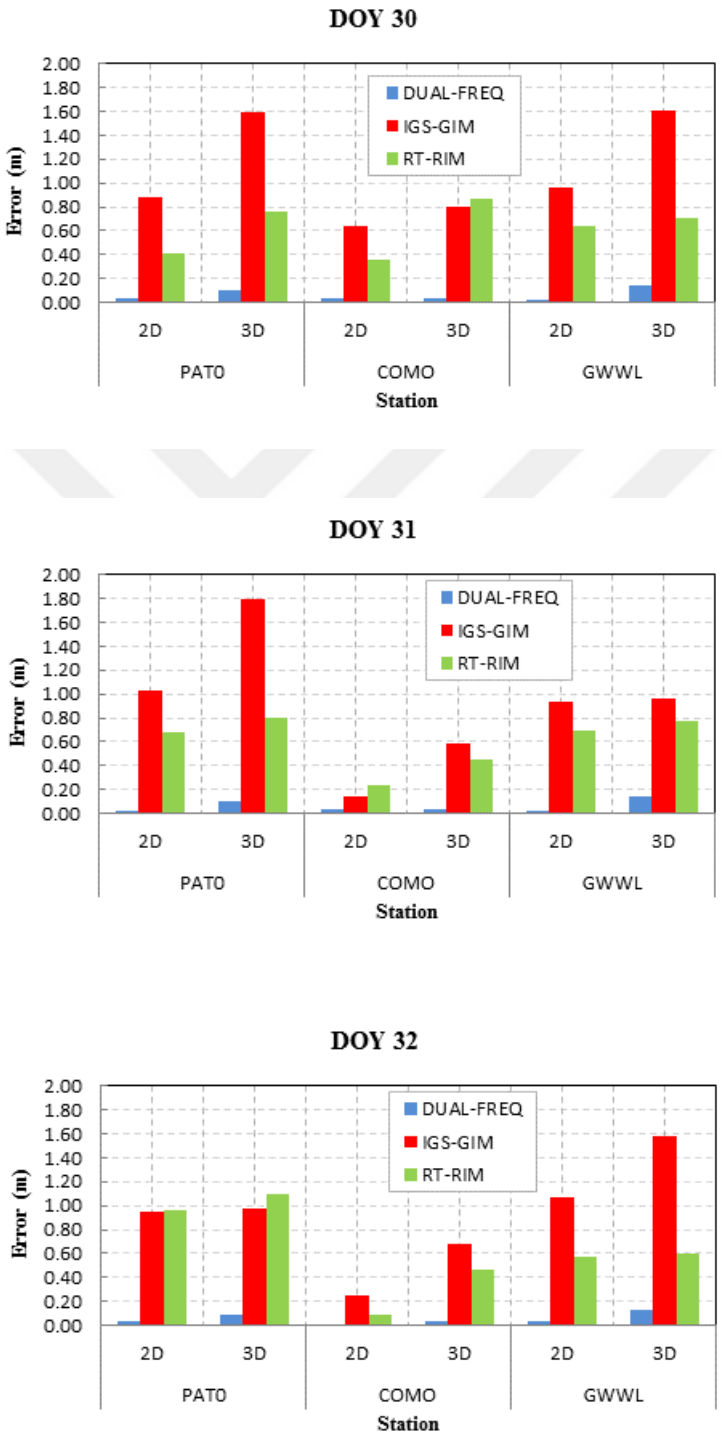

Figure 3.4 : 2D and 3D positioning accuracy.

Table 3.4 outlines the statistical parameters, including the mean, maximum, minimum and root mean square error (RMSE) values for the positioning accuracy of the single-frequency PPP obtained through the IGS-GIM and the RT-RIM, in comparison with the ionosphere-free dual frequency solution. The results show that the positioning accuracy obtained from the RT-RIM is more accurate than that of the IGS-GIM model

Table 3.4 : Statistical analysis for the positioning accuracy.

Statistical parameter (m)	IGS-GIM			RT-RIM		
	2D	H	3D	2D	H	3D
Mean	0.733	0.106	1.084	0.489	-0.057	0.631
Min.	0.104	-1.293	0.555	0.078	-0.618	0.411
Max.	1.039	1.373	1.699	0.923	0.786	0.999
RMSE	0.325	0.904	0.409	0.250	0.499	0.183

3.5 Conclusion

In this study, a real-time regional ionospheric model (RT-RIM) using the IGS-RTS precise satellite orbit and clock products has been developed. GPS observations from 60 IGS and EUREF reference stations over Europe have been processed using the Bernese 5.2 PPP module. The developed model has spatial and temporal resolution of 1° × 1° and 15 minutes, respectively. In order to evaluate the RT-RIM, the PPP convergence time and positioning accuracy for another set of stations over three consecutive days under high solar activity and one of them under active geomagnetic activity, have been estimated and compared with those of the IGS-GIM and ionosphere-free dual frequency counterparts. The findings show that the developed RT-RIM speeds up the convergence time. In addition the overall positioning accuracy has improved, under the mid-latitude region, typically by about 40%, 55% and 40% for the 2D, height and 3D components, respectively, with respect to the IGS-GIM counterpart.

4. MGR-DCB: A PRECISE MODEL FOR MULTI-CONSTELLATION GNSS RECEIVER DIFFERENTIAL CODE BIAS

4.1 Introduction

Global Navigation Satellite Systems (GNSS) have traditionally been used to investigate the spatio-temporal characteristics of the ionosphere Total Electron Content (TEC), both at the regional and the global levels. For precise estimation of the TEC, however, the Differential Code Bias (DCB) (i.e., difference in the code hardware delays at two different frequencies) for both of the satellites and the receiver must be accounted for. The satellite DCB values are stable over one day, while the receiver DCBs are not as stable (Sardon and Zarraoa, 1997; Schaer, 1999).

Earlier studies focused on the estimation of Global Positioning System (GPS) differential code bias (e.g., Arikan et al., 2008; Choi et al., 2011; Jin et al., 2012; Keshin, 2012; Kao et al., 2013). Keshin (2012) developed a model for receiver DCB estimation using vertical TEC values obtained from the IGS-GIM. The receiver DCBs and vertical residual ionospheric delays were computed using the least-squares estimation approach with linear constraints. The estimated values were compared with those of the IGS counterparts. The results showed agreement with the IGS values with differences less than 1 ns.

More recently, the DCBs for the new BeiDou and Galileo multi-GNSS signals were investigated by a number of researchers (e.g., Li et al., 2012; Montenbruck et al., 2014; Wei et al., 2014; Zhang et al., 2014). Montenbruck et al. (2014) developed the multi-GNSS DCB estimation model for both the receivers and satellites. The DCBs for the legacy and modernised GPS, Galileo and BeiDou signals were determined using data collected from the IGS-MGEX network. The IGS-GIM was used in order to remove the ionospheric contribution from the dual frequency pseudorange

This chapter is based on the paper: Abdelazeem, M., Çelik, R. N., & El-Rabbany, A. (2015). MGR-DCB: A Precise Model for Multi-constellation GNSS Receiver Differential Code Bias. *Journal of Navigation*, 1-11. doi: 10.1017/S0373463315000922.

differences. The estimated DCBs were compared with the group delay parameters transmitted through the GNSS broadcast ephemeris data. The findings showed good agreement with the broadcast parameters.

Ionospheric modelling using multi-GNSS measurements has been investigated by a number of researchers (e.g., Julien et al., 2012; Tu et al., 2013a; Tang et al., 2014; Zhang et al., 2015). In Zhang et al. (2015), a regional ionosphere delay model is built over China using data from BeiDou only, GPS only, and combined GPS/BeiDou. The results show that the combined GPS/BeiDou model can significantly improve the accuracy of the estimated TEC and DCBs.

The objective of this research is to develop a multi-frequency multi-GNSS receiver differential code bias model. The receiver DCBs for the legacy and modernised GPS, Galileo and BeiDou signals are estimated based on ionosphere-corrected geometry-free linear combinations of the pseudorange observations. One way to remove the ionospheric delay from the pseudorange differences is to use the IGS-GIM model (Montenbruck et al., 2014). Unfortunately, however, the IGS-GIM model has a limited spatiotemporal resolution. To overcome this problem, a Regional Ionospheric Model (RIM) over Europe is developed in this research. The developed RIM has spatial and temporal resolutions of 1° × 1° and 15 minutes, respectively. The accuracy of the developed RIM is validated for PPP applications. It is found that the positioning accuracy of the proposed RIM is superior to that of the IGS-GIM, where the RMSE values are reduced from ±0.325 to 0.25 m and from ±0.904 to 0.499 m, for the horizontal and height components, respectively (Abdelazeem et al., 2016a). In order to produce the RIM, GPS observations from a regional network consisting of 60 International GNSS Service (IGS) and EUREF reference stations are processed in the Bernese-5.20 PPP module in order to estimate the VTEC values. The resulting MGR-DCB model is validated for receiver DCBs estimation for three IGS-MGEX stations on three different days. The estimated DCBs are compared with the publicly available IGS-MGEX values. The findings reveal that the estimated DCBs have good agreement with the MGEX values with mean difference and RMSE values less than 1 ns. In addition, the combined GPS, BeiDou and Galileo VTEC are assessed and compared with the IGS-GIM counterparts. It is shown that the combined VTEC values have mean difference and RMSE values less than 1 TECU with respect to the IGS-GIM counterparts.

4.2 Proposed MGR-DCB Model Development

Firstly, a regional ionospheric model is developed in order to account for the effect of ionospheric delay in the pseudorange difference equations. The basic GPS observation equations can be expressed as follows (Kleusberg and Teunissen, 1998):

$$P_i = \rho_r^s + c(dt_r - dt^s) + I_{r,i}^s + T_r^s + c\left(d_{r,i} + d_i^s\right) + \varepsilon_{p,i} \tag{4.1}$$

$$\varphi_i = \rho_r^s + c(dt_r - dt^s) - I_{r,i}^s + T_r^s + c\left(\delta_{r,i} + \delta_i^s\right) + \lambda_i N_i + \varepsilon_{\varphi,i} \tag{4.2}$$

where P_i and φ_i are the pseudorange and carrier phase measurements in meter, respectively; ρ_r^s is the satellite-receiver true geometric range; c is the speed of light in vacuum; dt_r and dt^s are the receiver and satellite clock errors, respectively; $I_{r,i}^s$ the ionospheric delay; T_r^s the tropospheric delay; $d_{r,i}$ and d_i^s are the code hardware delay for the receiver and the satellite, respectively; $\delta_{r,i}$ and δ_i^s are the carrier phase hardware delay for the receiver and the satellite, respectively; λ_i is the wavelength of carrier phase; N_i is the non-integer phase ambiguity, and $\varepsilon_{p,i}$ and $\varepsilon_{\varphi,i}$ are the code and phase unmodeled errors, including noise and multipath.

Geometry-free linear combinations are formed using the un-differenced carrier smoothed code observations, which eliminate the geometrical term, tropospheric delay, receiver and satellite clock errors as follows (Dach et al., 2007):

$$P_4 = P_2^- - P_1^- = \left(\frac{f_1^2}{f_2^2} - 1\right) I_r^s - c(DCB_r + DCB^s) \tag{4.3}$$

where P_i^- is the smoothed code observables; I_r^s is the L1 ionospheric delay; c is the light speed in vacuum; DCB_r and DCB^s are the differential code bias for the receiver and the satellite, respectively.

Based on Equation (4.3), the Slant TEC (STEC) along the satellite-receiver path can be determined as follows:

$$STEC = \left(\frac{f_1^2 f_2^2}{40.3(f_1^2 - f_2^2)}\right)[P_4 + c\,(DCB_r + DCB^s)] \tag{4.4}$$

The Vertical TEC (VTEC) can be estimated using the Modified Single Layer Model (MSLM) mapping function, which assumes that all free electrons are concentrated in

a shell of infinitesimal thickness at height H. The effective height (H) corresponds to maximum electron density at the F2 peak ranges from 350 km to 450 km. The VTEC is determined at the Ionosphere Pierce Point (IPP), the point of intersection between the shell layer and satellite-receiver path, as given below (Schaer, 1999):

$$VTEC = STEC * cos\left(arcsin\left(\frac{R}{R+H} sin(\alpha z)\right)\right) \tag{4.5}$$

where z is the satellite's zenith distance at the receiver; R is the mean radius of the Earth, and α is a correction factor. Best fit of the MSLM with respect to the JPL Extended Slab Model (ESM) mapping function is achieved at $H = 506.76\,km$ and $\alpha = 0.9782$, when using $R = 6371\,km$ and assuming a maximum zenith distance of 80 degrees (Dach et al., 2007).

The VTEC can be modeled on a regional scale as a function E(β, s) of the geographic latitude (β) and the sun-fixed (s) longitude of the IPP, respectively. The regional VTEC is expressed as a spherical harmonic expansion, which takes the form (Schaer, 1999):

$$E(\beta, s) = \sum_{n=0}^{n_{max}} \sum_{m=0}^{n} P_{nm}^{-}(sin\,\beta)\,(a_{nm}\,cos\,ms + b_{nm}\,sin\,ms) \tag{4.6}$$

where n_{max} is the maximum degree of the spherical harmonic expansion; P_{nm}^{-} are normalized associated Legendre functions of degree n and order m; a_{nm} and b_{nm} are the unknown coefficients of spherical harmonics.

Substituting Equations (4.4) and (4.5) into Equation (4.6), the ionospheric spherical harmonic model can be expressed as:

$$\begin{aligned} &\sum_{n=0}^{n_{max}} \sum_{m=0}^{n} P_{nm}^{-}(sin\,\beta)\,(a_{nm}\,cos\,ms + b_{nm}\,sin\,ms) \\ &\quad = \left(\frac{f_1^2 f_2^2}{40.3(f_1^2 - f_2^2)}\right)[P_4 + c\,(DCB_r + DCB^s)] \\ &\quad * \; cos\left(arcsin\left(\frac{R}{R+H} sin(\alpha z)\right)\right) \end{aligned} \tag{4.7}$$

where a_{nm}, b_{nm}, DCB_r and DCB^s are the unknowns parameters to be computed.

In order to separate the DCBs of the receivers and satellites, an additional constraint must be used. It assumes that the sum of satellite DCBs is zero as follows (Dach et al., 2007):

$$\sum_{s=1}^{s=max} \Delta b^s = 0 \tag{4.8}$$

After the development of the RIM, the multi constellation GNSS receiver DCB can be estimated through the use of Equations 4.4 and 4.5 as follows:

$$DCB_r = \left(\frac{40.3(f_1^2 - f_2^2)}{c\, f_1^2 f_2^2}\right) VTEC * MF - \left(\frac{P_2 - P_1}{c}\right) - DCB^s \tag{4.9}$$

$$MF = \left[cos\left(arcsin\left(\frac{R}{R+H} sin(z)\right)\right)\right]^{-1} \tag{4.10}$$

where MF is the mapping function; P_1 and P_2 are the code observations on L_1 and L_2, respectively; f_1 and f_2 are the carrier phase frequencies on L_1 and L_2, respectively; The VTEC values are extracted from the RIM file for every 15 minutes. In addition, the satellite DCBs are obtained from the available MGEX file. The receiver DCBs is computed every 15 minutes, thus the daily average value can be obtained as follows:

$$DCB_{r,avg} = \frac{1}{n} \sum_{i=1}^{i=n} DCB_r \tag{4.11}$$

The developed MGR-DCB model uses the unsmoothed code observations, where there is no effect of the noise level on the estimated daily mean differential code bias values (Montenbruck et al., 2014).

In order to validate the developed MGR-DCB model, the combined VTEC is computed from the GPS, BeiDou and Galileo measurements by mapping the STEC from the high elevation satellites and assuming a single VTEC for each epoch. The combined VTEC can be obtained as follows (Tang et al., 2014):

$$B = AX \tag{4.12}$$

$$\begin{bmatrix} P_4 + cDCB_r + cDCB^{s=1} \\ \vdots \\ P_4 + cDCB_r + cDCB^{s=n} \end{bmatrix} = \begin{bmatrix} k * MF^{s=1} \\ \vdots \\ k * MF^{s=n} \end{bmatrix} [VTEC] \tag{4.13}$$

where n is the number of the observed GPS, BeiDou or Galileo satellites with high elevation angle into the single epoch; k is a frequency-dependent factor, $k = \frac{40.3(f_1^2 - f_2^2)}{(f_1^2 f_2^2)}$. It should be pointed out that the factor k has three different values for the each of the GPS, BeiDou and Galileo systems.

The combined VTEC is estimated from high elevation satellites under the assumption that the computed VTEC from those satellites are approximately equal to the VTEC values at the zenith above the receiver.

4.3 Methodology

A regional network consisting of 60 IGS and EUREF reference stations in Europe has been used to develop the regional ionospheric model (Figure 4.1). The stations are homogeneously distributed in different latitudes in order to reflect different ionospheric characteristics. GPS observations for three different days (Day of Year (DOY) 130, 200 and 362 in year 2014) have been downloaded (BKG, 2015) to represent the ionosphere seasonal variations in May, August and December, respectively. Each observation file has a 24-hour time span and a 30-second time interval. An elevation cut-off angle of 20° has been used. The files have been processed using the PPP module in the Bernese-5.20 software package. In order to produce the RIM, the IGS final satellite orbit, satellite clock and earth orientation parameters have been used (IGS, 2015) and then have been converted into the Bernese formats. The un-differenced code observations have been smoothed. In the parameters estimation process, the effective height has been selected to be 450 km. In addition, a maximum degree and order equal to six of the spherical harmonic expansions have been selected with a 15-minute interval. A group of 49 coefficients of the spherical harmonic model has been obtained each time epoch. Thereafter, to extract the VTEC maps a spatial and temporal resolution of 1° × 1° and 15 minutes, respectively, have been selected.

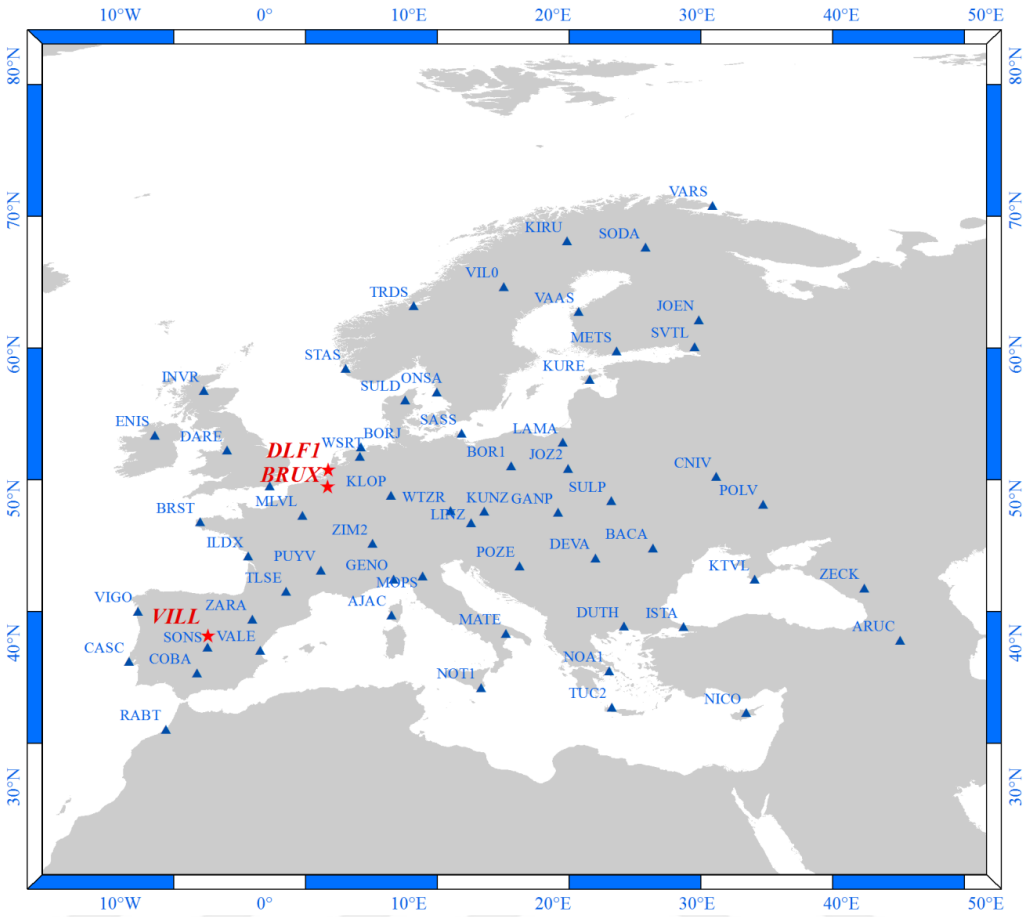

Figure 4.1 : Reference stations distribution (with triangle shape) and examined stations (with asterisk shape).

In order to estimate the receiver differential code bias, The MGR-DCB model has been developed. A FORTRAN code has been written as per the flowchart shown in Figure 4.2. The VTEC values have been extracted from the RIM file at a 15-minute time interval. The estimation of the satellite DCB needs a well-distributed network, however, only three stations have been examined, therefore the satellite DCBs available from MGEX website (MGEX, 2015) has been used.

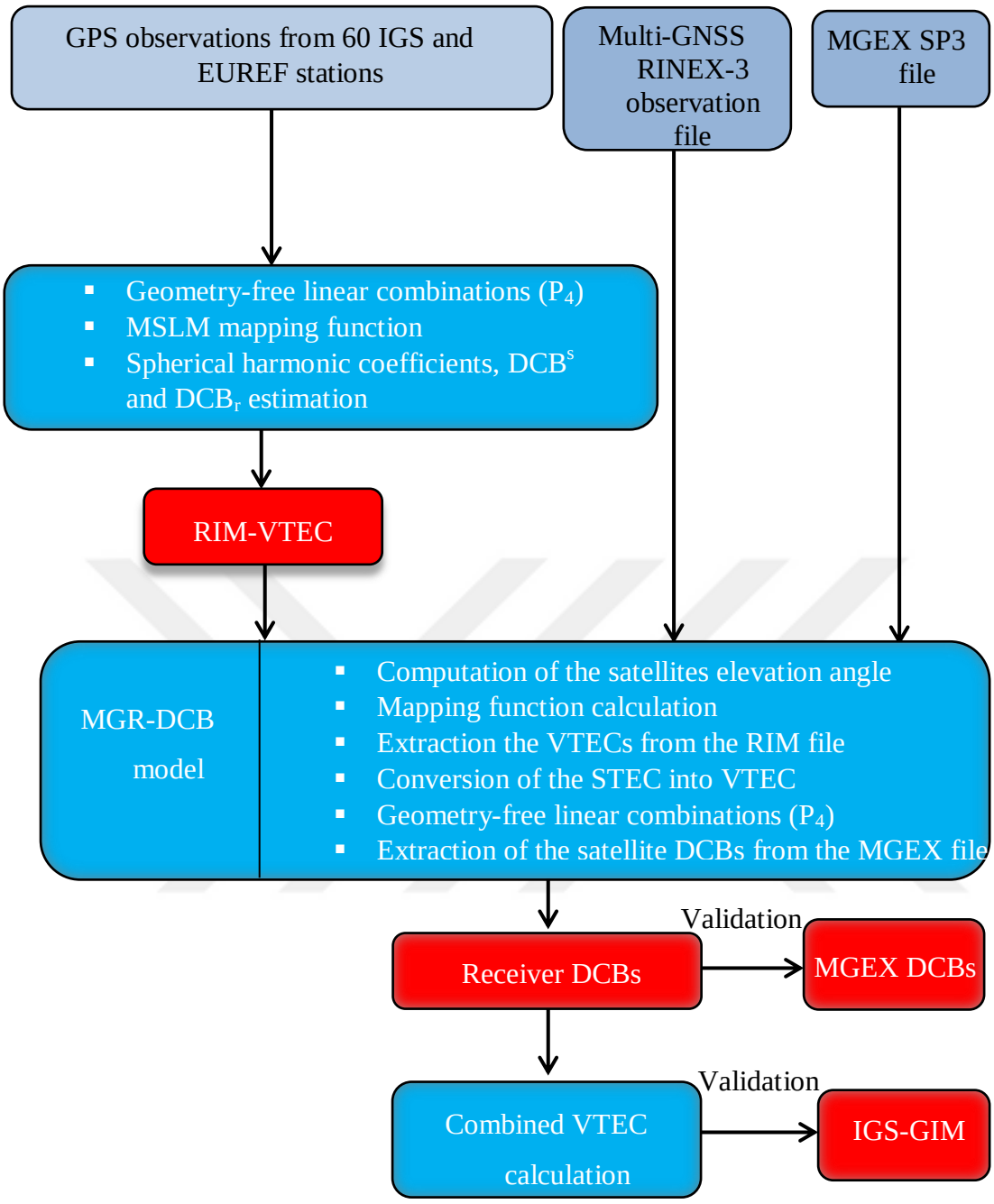

Figure 4.2: Flow chart of the developed MGR-DCB.

4.4 Results and Analysis

In order to assess the developed MGR-DCB model, the receiver DCBs for another set of reference stations was computed (Figure 4.1). The DCBs for the EUREF stations were not available, therefore only the MGEX stations were examined. The examined stations were selected to represent different latitudes and receiver types (Table 4.1). The legacy GPS DCBs for the P(Y)-code on the L1 and L2 tracking signals (C1W-C2W) was assessed. In addition, the DCBs for the GPS L1 C/A

tracking and the L2 P(Y) tracking (C1C-C2W) was computed. Thereafter, the DCBs for the modernised GPS civil L5 signal with the different tracking mode used by the MGEX receivers (i.e., C1C-C5Q and C1C-C5X) were determined. For the BeiDou system, the DCBs for the three signals B1, B2 and B3 (C2I-C6I and C2I-C7I) were evaluated. For the Galileo E1, E5a, E5b and E5 signals, the DCBs for the receiver pilot-tracking mode, indicated by C1C-C5Q, C1C-C7Q and C1C-C8Q were determined. In addition, the C1X-C5X, C1X-C7X and C1X-C8X DCBs for the receiver combined (pilot and data) tracking mode were estimated.

Table 4.1 : Examined stations characteristics.

Station	Latitude	Longitude	Receiver type	Antenna type
VILL	40.4436	356.0480	SEPT POLARX4	SEPCHOKE_MC NONE
BRUX	50.7980	4.3585	SEPT POLARX4TR	JAVRINGANT_DM NONE
DLF1	51.9860	4.3875	TRIMBLE NETR9	LEIAR25.R3 LEIT

Table 4.2 outlines the estimated multi-GNSS receiver DCBs for the examined stations in the three days and for the different receiver tracking modes. It is shown that the estimated DCBs from the MGR-DCB model have good agreement with the IGS-MGEX values.

Figure 4.3 shows the mean difference and the RMSE of the receiver DCBs obtained from the MGR-DCB with respect to the IGS-MGEX DCBs values. For the legacy GPS C1W-C2W DCBs, it is shown that the mean difference is about -0.31 ns and 0.11 ns for station VILL and BRUX, respectively. For their RMSE values, they are about ±0.14 ns and 0.08 ns, respectively. The mean difference of the C1C-C2W DCB for station DLF1 is about 0.21 ns with ±0.08 ns RMSE value. For the modernised GPS L5 signal, the discrepancy between the estimated and MGEX is about -0.12 ns, 0.34 ns and 0.34 ns for station VILL, BRUX and DLF1, respectively. In addition, the RMSE values are about ±0.06, 0.23 and 0.33 ns for station VILL, BRUX and DLF1, respectively.

Table 4.2 : Estimated DCB values.

DCB	Station	DOY 130		DOY 200		DOY 362	
		MGEX (ns)	Estimated (ns)	MGEX (ns)	Estimated (ns)	MGEX (ns)	Estimated (ns)
GPS							
C1W-C2W	BRUX	8.80	8.63	8.15	7.98	8.09	8.10
	VILL	6.22	6.55	5.22	5.36	4.98	5.45
C1C-C2W	DLF1	-17.38	-17.70	-17.79	-17.99	-17.97	-18.09
C1C-C5Q	BRUX	-1.38	-2.04	-2.82	-3.06	-0.88	-1.00
	VILL	-2.62	-2.53	-4.17	-4.11	-4.08	-3.88
C1C-C5X	DLF1	-17.60	-18.42	-18.83	-18.93	-19.16	-19.28
BeiDou							
C2I-C7I	BRUX	19.35	19.66	19.28	18.54	20.55	20.41
	VILL	16.52	15.94	15.75	14.98	16.70	17.53
C2I-C6I	DLF1	45.35	45.04	44.74	43.88	46.19	45.59
C2I-C7I	DLF1	21.53	21.20	21.14	20.35	23.04	22.52
Galileo							
C1C-C5Q	BRUX	1.06	0.13	1.26	1.40	2.88	2.91
	VILL	0.14	-0.03	-0.59	0.24	-0.43	0.29
C1C-C7Q	BRUX	12.62	11.72	12.70	12.74	13.04	13.07
	VILL	10.54	10.33	9.93	10.67	10.08	10.67
C1C-C8Q	BRUX	8.74	7.93	9.01	9.14	9.78	9.72
	VILL	7.39	7.30	6.88	7.58	6.99	7.65
C1X-C5X	DLF1	-0.47	-0.81	0.27	0.09	-0.46	-0.66
C1X-C7X	DLF1	1.77	2.04	2.46	2.35	2.41	2.78
C1X-C8X	DLF1	-0.16	-1.13	0.73	0.15	0.35	0.51

The BeiDou (C2I-C7I) differential code bias estimated from the MGR-DCB model show offsets from the MGEX values about 0.17, 0.19 and 0.55 ns with RMSE values about ±0.71, 0.43 and 0.19 ns for stations VILL, BRUX and DLF1, respectively. The BeiDou B3 signal can be tracked by station DLF1, thus its C2I-C6I DCB shows a mean difference of 0.59 ns with a RMSE value of ±0.22 ns.

The resulting Galileo E1-E5a differential code biases exhibit mean differences from the MGEX values about -0.46, 0.26 and 0.24 ns for stations VILL, BRUX and DLF1, respectively. In addition, the RMSE of the VILL, BRUX and DLF1 are ±0.45, 0.48 and 0.07 ns, respectively. For the resulting E1-E5b DCBs, the mean discrepancies are -0.37, 0.28 and -0.17 ns, while the RMSE values are ±0.42, 0.44 and 0.20 ns for stations VILL, BRUX and DLF1, respectively. The mean differences for the estimated E1-E5 DCBs are -0.42, 0.25 and 0.46 ns with RMSE values ±0.36, 0.41 and 0.47 ns for stations VILL, BRUX and DLF1, respectively.

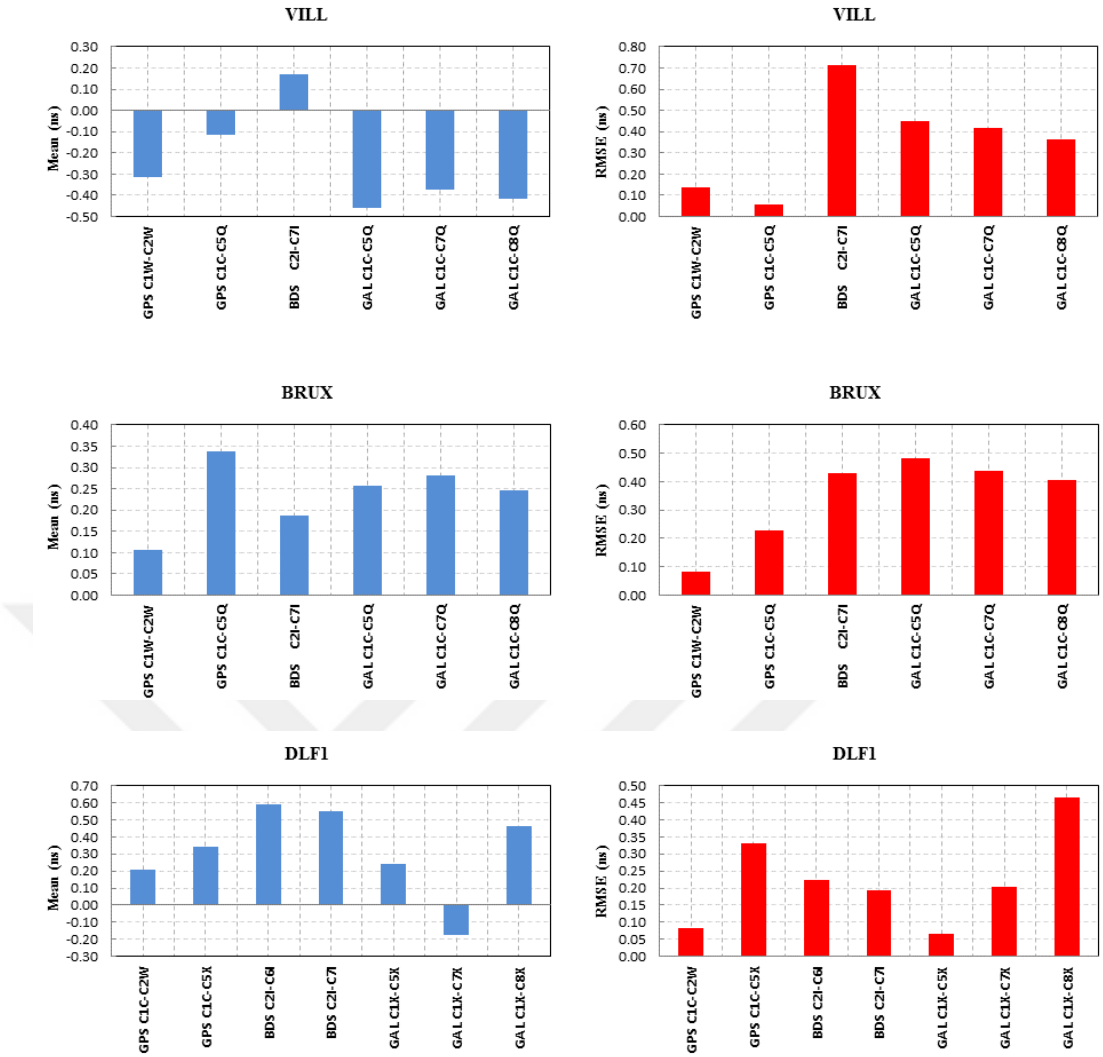

Figure 4.3 : DCBs mean and RMSE values.

It is shown from the above results that the mean difference between the estimated receiver DCBs and MGEX counterparts is less than 1 ns. In addition, the RMSE for the three examined stations is also less than 1 ns. This level of agreement means that the ionospheric correction values obtained through the developed regional ionospheric model are accurate. However, the station location contributes to the accuracy of the computed ionospheric value. This appears for station DLF1, where the mean difference is large (Figure 4.3). This is due to the fact that station DLF1 is located at the border of the developed ionospheric model as shown in Figure 4.1.

In order to validate the model, the Combined Vertical Total Electron Content (CVTEC) are computed from the GPS, Galileo and BeiDou measurements and then compared with the IGS-GIM counterparts. For illustration purposes, only the VTEC

profiles for stations VILL, BRUX and DLF1, respectively on DOY 130 are given in Figure 4.4.

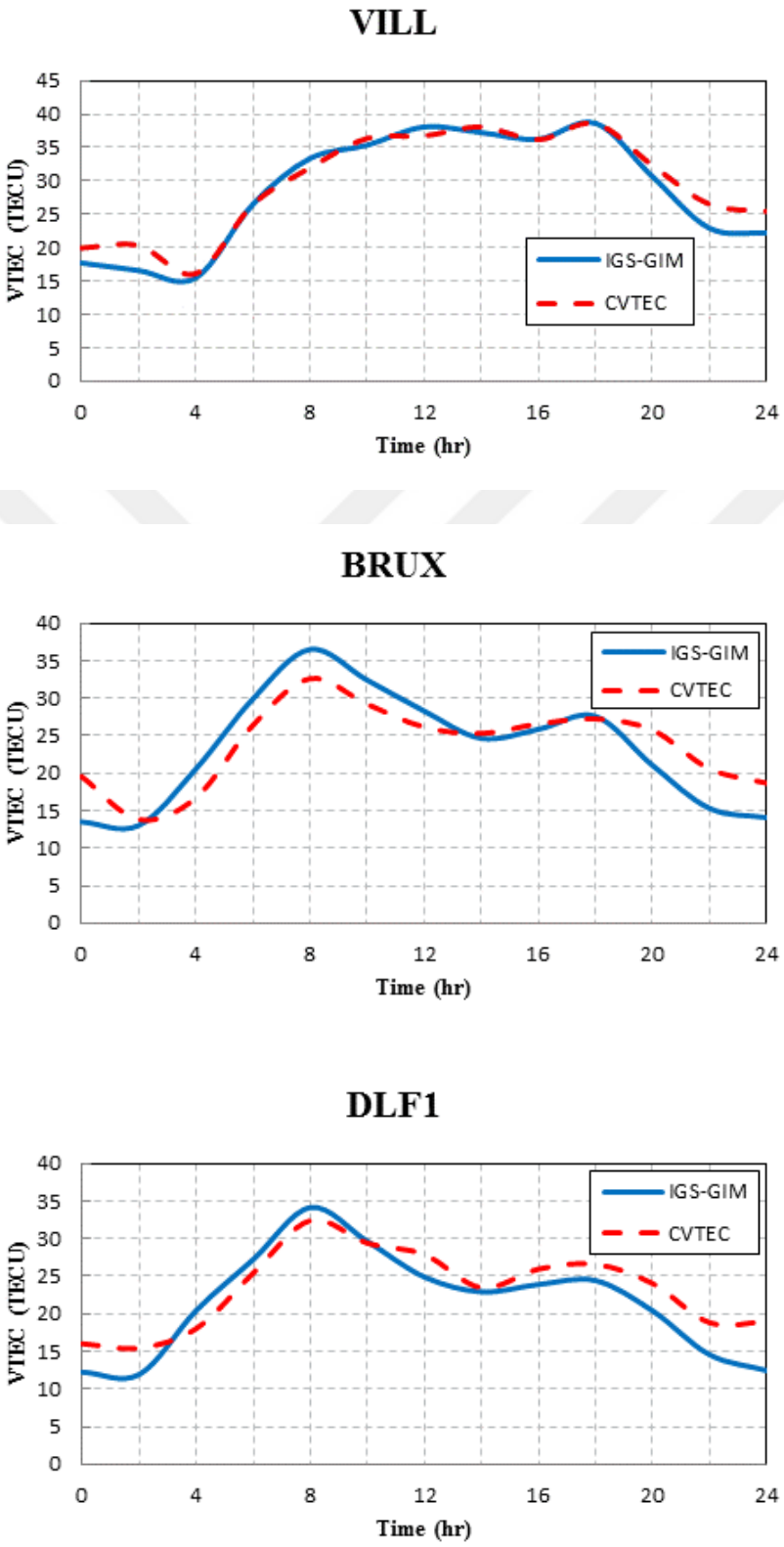

Figure 4.4 : VTEC profiles on DOY 130.

Figure 4.5 illustrates the mean differences and RMSE values of the CVTEC with respect to the IGS-GIM counterparts for the three examined stations. It is shown that for station VILL the mean difference is about 0.4226 TECU with RMSE value about ±0.5833 TECU. For station BRUX, the mean discrepancy is -0.2454 TECU, while the RMSE is ±0.8528 TECU. In addition, the mean difference and RMSE values for station DLF1 are 0.8259 TECU and ±0.6881 TECU, respectively.

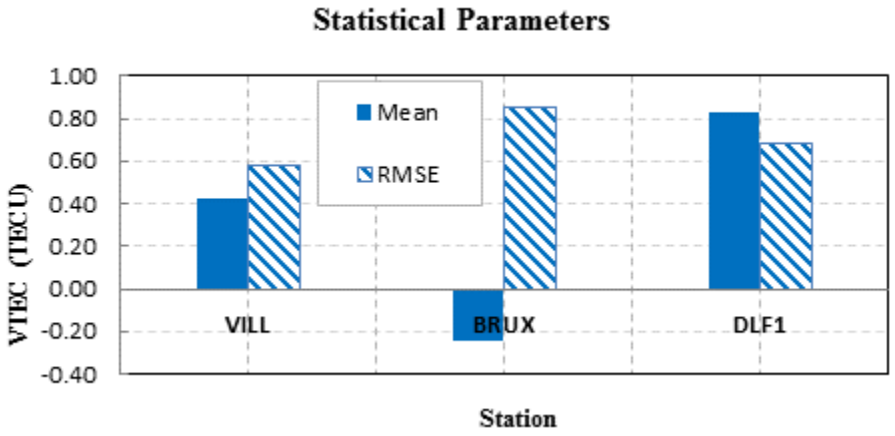

Figure 4.5 : Statistical parameters for the CVTEC differences.

4.5 Conclusion

In this paper, a Multi-frequency multi-GNSS Receiver Differential Code Bias estimation model has been developed using the ionosphere-corrected geometry-free linear combinations of the pseudorange observations. In order to correct the pseudorange differences from the ionospheric delay, a Regional Ionospheric Model over Europe has been developed using GPS observations. The developed RIM has spatial and temporal resolutions of 1° × 1° and 15 minutes, respectively. To validate the proposed model, the receiver DCBs for GPS, Galileo and BeiDou signals have been estimated for three MGEX stations over three different days. It has been shown that the estimated DCBs have good agreement with the MGEX values, with mean difference and RMSE values less than 1 ns. In addition, the combined GPS, BeiDou and Galileo VTEC have been assessed and compared with the IGS-GIM counterparts. The findings showed good agreement with the IGS-GIM values with mean difference and RMSE values less than 1 TECU.

5. CONCLUSION AND RECOMMENDATIONS

5.1 Conclusion

The main objective of this study was to develop a regional ionospheric delay correction model for single-frequency precise point positioning users in Europe. The spatial and temporal resolutions of the newly developed model were 1° × 1° and 15 minutes, respectively. GNSS observations from a regional network consisting of a number of IGS and EUREF stations were used. The model was developed for post processing (i.e., RIM) and real-time (i.e., RT-RIM) applications. The recently launched IGS-RTS satellite orbit and clock products were used in order to produce the RT-RIM. In order to validate the resulting RIMs, single-frequency PPP convergence time and positioning accuracy for another set of stations were estimated and compared with those of the IGS-GIM counterparts. Ionosphere-free dual frequency PPP was used as reference.

A multi-constellation GNSS receiver differential code bias estimation model was also developed. The receiver DCBs for GPS, Galileo and BeiDou signals were estimated using the ionosphere-corrected geometry-free linear combinations of the code observations. A regional ionospheric model over Europe was developed in order to mitigate the ionospheric delay from the pseudorange differences. The developed RIM has a spatial and temporal resolution of 1° × 1° and 15 minutes, respectively. To validate the proposed MGR-DCB model, the receiver DCB values for three MGEX stations were estimated and compared with the MGEX counterparts.

It has been shown that the developed RIMs achieve a decimetre-level positioning accuracy and accelerated the convergence time. The positioning accuracy of the developed RIMs was found superior to that of the IGS-GIM, particularly in the height component. The proposed RIM, for instance, improved the PPP accuracy by about 20%, 45% and 45% for the 2D, height and 3D components, respectively, in comparison with the IGS-GIM model. For the newly developed RT-RIM, the PPP accuracy was also improved by about 40%, 55% and 40% for the horizontal, height

and 3D components, respectively, with respect to the IGS-GIM counterparts. Therefore, this promising positioning accuracy can be used in many applications, including GIS, hydrographic survey and remote sensing applications.

For the proposed MGR-DCB model, the results showed that the estimated receiver DCB values have good agreement with the IGS-MGEX counterparts, with mean difference and RMSE values less than 1 ns. In addition, combined GPS, Galileo and BeiDou VTEC values showed good agreement with the IGS-GIM counterparts, with mean difference and RMSE values less than 1 TECU. As a result, the developed MGR-DCB can be used for precise ionosphere monitoring and space weather applications.

5.2 Recommendations

A number of points can be given for further investigations:

- Developing a RT-RIM using the IGS-RTS products for other systems (i.e., Galileo and BeiDou).
- Developing a real-time MGR-DCB model using the IGS-RTS products.
- For the MGR-DCB development, using a physical model (e.g., NeQuick or IRI models) to remove the ionospheric delay from the pseudorange differences, as opposed to the RIM, should be investigated.

REFERENCES

Abdelazeem, M., Çelik, R. N., & El-Rabbany, A. (2016a). An Enhanced Real-Time Regional Ionospheric Model Using IGS Real-Time Service (IGS-RTS) Products. *Journal of Navigation*, *69(3)*, 521-530.

Abdelazeem, M., Çelik, R. N., & El-Rabbany, A. (2016b). An improved regional ionospheric model for single-frequency GNSS users. *Survey Review*, 1-7. doi: 10.1080/00396265.2016.1138581.

Abdelazeem, M., Çelik, R. N., & El-Rabbany, A. (2015). MGR-DCB: A Precise Model for Multi-constellation GNSS Receiver Differential Code Bias. *Journal of Navigation*, 1-11. doi: 10.1017/S0373463315000922.

Alothman, A. O., Alsubaie, M. A., & Ayhan, M. E. (2011). Short term variations of total electron content (TEC) fitting to a regional GPS network over the Kingdom of Saudi Arabia (KSA). *Advances in Space Research, 48*(5), 842-849.

Arikan, F., Nayir, H., Sezen, U., & Arikan, O. (2008). Estimation of single station interfrequency receiver bias using GPS-TEC. *Radio Science, 43*(4), RS4004 (13 pp.).

Bhuyan, P. K., & Borah, R. R. (2007). TEC derived from GPS network in India and comparison with the IRI. *Advances in Space Research, 39*(5), 830-840.

BKG (2015). Agency for Cartography and Geodesy, ftp://igs.bkg.bund.de/, accessed on 01.04.2015.

Caissy, M., Agrotis, L., Weber, G., Hernandez-Pajares, M. & Hugentobler, U. (2012). The international GNSS real-time service. *GPS World, 23*(6)**,** 52-58.

Chen, J., Ge, M., Dousa, J., Gendt, G. & Ramatschi, M. (2010). Evaluating and improving GNSS real-time positioning using IGS-RTPP products for tsunami early warning system. *IGS Workshop and Vertical Rates Symposium*, Newcastle, England.

Chen, J., Li, H., Wu, B., Zhang, Y., Wang, J., & Hu, C. (2013). Performance of Real-Time Precise Point Positioning. *Marine Geodesy, 36*(1), 98-108.

Choi, B. K., Cho, J. H., & Lee, S. J. (2011). Estimation and analysis of GPS receiver differential code biases using KGN in Korean Peninsula. *Advances in Space Research, 47*(9), 1590-1599.

Dach, R., Hugentobler, U., Fridez, P., & Meindl, M. (2007). Bernese GPS Software Version 5.0. Astronomical Institute, University of Berne (AIUB).

Durmaz, M. (2013). Non-Parametric and Semi-Parametric Regional Modeling of the Ionospheric Vertical Total Electron Content Using Ground-Based GPS Observations. *Ph.D. Thesis*, Middle East Technical University, Turkey.

Durmaz, M., & Karslioglu, M. O. (2015). Regional vertical total electron content (VTEC) modeling together with satellite and receiver differential code biases (DCBs) using semi-parametric multivariate adaptive regression B-splines (SP-BMARS). *Journal of Geodesy, 89*(4), 347-360.

Durmaz, M., Karslioglu, M. O., & Nohutcu, M. (2010). Regional VTEC modeling with multivariate adaptive regression splines. *Advances in Space Research, 46*(2), 180-189.

El-Rabbany, A. (2006). *Introduction to GPS: The Global Positioning System*. Boston: Artech House.

Gao, S. (2007). Monitoring and Modelling Hong Kong Ionosphere Using Regional GPS Networks. *Ph.D. Thesis*, Hong Kong Polytechnic University, Hong Kong.

GFZ (2015). German Research Center for Geoscience, http://www.gfz-potsdam.de/en/research/organizationalunits/departments/department-2/earths-magnetic-field/services/kp-index/, accessed on 15.02.2015.

Guo, F., Zhang, X., & Wang, J. (2015). Timing group delay and differential code bias corrections for BeiDou positioning. *Journal of Geodesy, 89*(5), 427-445.

Hadas, T., & Bosy, J. (2015). IGS RTS precise orbits and clocks verification and quality degradation over time. *GPS Solutions, 19*(1), 93-105.

Hofmann-Wellenhof, B., Lichtenegger, H., & Wasle, E. (2008). *GNSS - Global Navigation Satellite Systems: GPS, GLONASS, Galileo & more*. Wien: Springer Wien NewYork.

Hunsucker, R. D., & Hargreaves, J. K. (2003). *The high-latitude ionosphere and its effects on radio propagation*. Cambridge: Cambridge University Press.

IGS (2015). International GNSS Service, ftp://cddis.gsfc.nasa.gov/, accessed on 01.04.2015.

IGS-RTPP (2015). International GNSS Service Real Time Pilot Project, ftp://cddis.gsfc.nasa.gov/gps/products/rtpp/, accessed on 15.02.2015.

Jin, R., Jin, S., & Feng, G. (2012). M_DCB: Matlab code for estimating GNSS satellite and receiver differential code biases. *GPS Solutions, 16*(4), 541-548.

Julien, O., Issler, J.-L., & Lestarquit, L. (2012). Ionospheric delay estimation using Galileo E5 signals only. *25th International Technical Meeting of the Satellite Division of the Institute of Navigation, ION GNSS 2012*, Nashville, TN, United states, Septmeber 17-21.

Kao, S.-P., Chen, Y.-C., & Ning, F.-S. (2014). A MARS-based method for estimating regional 2-D ionospheric VTEC and receiver differential code bias. *Advances in Space Research, 53*(2), 190-200.

Kao, S., Tu, Y., Chen, W., Weng, D. J., & Ji, S. Y. (2013). Factors affecting the estimation of GPS receiver instrumental biases. *Survey Review, 45*(328), 59-67.

Kaplan, E. D. & Hegarty, C. J. (2006). *Understanding GPS Principles and Applications.* 2nd Edition. Boston: Artech House.

Kelley, M. C. (2009). *The earth's ionosphere: plasma physics and electrodynamics*. Burlington: Academic Press, Elsevir.

Keshin, M. (2012). A new algorithm for single receiver DCB estimation using IGS TEC maps. *GPS Solutions, 16*(3), 283-292.

Kleusberg, A., & Teunissen, P.J.G. Eds (1998). *GPS for Geodesy*. 2nd Edition, Berlin: Springer-Verlag.

Klobuchar, J. A. (1987). IONOSPHERIC TIME-DELAY ALGORITHM FOR SINGLE-FREQUENCY GPS USERS. *IEEE Transactions on Aerospace and Electronic Systems, AES-23*(3), 325-331.

Kouba, J. (2009). A guide to Using International GNSS Service (IGS) Products. Available from https://igscb.jpl.nasa.gov/igscb/resource/pubs/UsingIGSProductsVer21.pdf.

Li, X., Guo, B., Lu, C., Ge, M., Wickert, J., & Schuh, H. (2014). Real-time GNSS seismology using a single receiver. *Geophysical Journal International, 198*(1), 72-89.

Li, Z., Yuan, Y., Li, H., Ou, J., & Huo, X. (2012). Two-step method for the determination of the differential code biases of COMPASS satellites. *Journal of Geodesy, 86*(11), 1059-1076.

Li, Z., Yuan, Y., Wang, N., Hernandez-Pajares, M., & Huo, X. (2015). SHPTS: towards a new method for generating precise global ionospheric TEC map based on spherical harmonic and generalized trigonometric series functions. *Journal of Geodesy, 89*(4), 331-345.

Liu, J., Chen, R., Wang, Z., & Zhang, H. (2011). Spherical cap harmonic model for mapping and predicting regional TEC. *GPS Solutions, 15*(2), 109-119.

Memarzadeh, Y. (2009). Ionospheric Modeling for Precise GNSS Applications. *Ph.D. Thesis*, Delft University of Technology, Netherland.

MGEX (2015). IGS Multi-GNSS Experiment, ftp://cddis.gsfc.nasa.gov/gps/products/mgex, accessed on 01.04.2015.

Montenbruck, O., Hauschild, A., & Steigenberger, P. (2014). Differential code bias estimation using multi-GNSS observations and global ionosphere maps. *Institute of Navigation International Technical Meeting, ITM 2014*, San Diego, CA, United states, Januray 27-29.

Nava, B., Coisson, P., & Radicella, S. M. (2008). A new version of the NeQuick ionosphere electron density model. *Journal of Atmospheric and Solar-Terrestrial Physics, 70*(15), 1856-1862.

NICT-SWIC (2015). NICT Space Weather Information Center, http://swc.nict.go.jp/sunspot/latest30sunspot_e.php, accessed on 15.02.2015.

Nohutcu M. (2009). Development of a Matlab Based Software Package for Ionosphere Modeling. *Ph.D. Thesis*, Middle East Technical University, Turkey.

Nohutcu, M., Karslioglu, M. O., & Schmidt, M. (2010). B-spline modeling of VTEC over Turkey using GPS observations. *Journal of Atmospheric and Solar-Terrestrial Physics, 72*(7-8), 617-624.

Ohashi, M., Otsuki, S., Okano, N., Kubo, Y., & Sugimoto, S. (2011). Local models for ionospheric VTEC estimation based on GR models with multi-layer models. *24th International Technical Meeting of the Satellite Division of the Institute of Navigation, ION GNSS 2011*, Portland, United states, September 19-23.

Oladipo, O. A., & Schuler, T. (2012). GNSS single frequency ionospheric range delay corrections: NeQuick data ingestion technique. *Advances in Space Research, 50*(9), 1204-1212. doi:10.1016/j.asr.2012.06.035

Opperman, B. D. L., Cilliers, P. J., McKinnell, L.-A., & Haggard, R. (2007). Development of a regional GPS-based ionospheric TEC model for South Africa. *Advances in Space Research, 39*(5), 808-815.

Prolss, G. W. (2004). *Physics of the Earth's space environment: An introduction*. Berlin: Springer.

Rovira-Garcia, A., Juan, J. M., Sanz, J., & Hernandez-Pajares, M. (2012). Fast precise point positioning performance based on international GNSS real-time service data. *6th ESA Workshop on Satellite Navigation Technologies: Multi-GNSS Navigation Technologies Galileo's Here, NAVITEC 2012 and European Workshop on GNSS Signals and Signal Processing*, Noordwijk, Netherlands, December 5-7.

Sardon, E., & Zarraoa, N. (1997). Estimation of total electron content using GPS data: How stable are differential satellite and receiver instrumental biases?. *Radio Science, 32*(5), 1899-1910.

Schaer, S. (1999). Mapping and Predicting the Earth's Ionosphere Using the Global Positioning System. *Ph.D. Thesis*, University of Bern, Switzerland.

Schunk, R. W., & Nagy, A. F. (2009). *Ionospheres: Physics, plasma physics, and chemistry*. 2nd Edition. Cambridge: Cambridge University Press.

Tang, W., Jin, L., & Xu, K. (2014). Performance Analysis of Ionosphere Monitoring with BeiDou CORS Observational Data. *Journal of Navigation, 67*(03), 511-522.

Tu, R., Ge, M., Zhang, H., & Huang, G. (2013a). The realization and convergence analysis of combined PPP based on raw observation. *Advances in Space Research, 52*(1), 211-221.

Tu, R., Zhang, H., Ge, M., & Huang, G. (2013b). A real-time ionospheric model based on GNSS Precise Point Positioning. *Advances in Space Research, 52*(6), 1125-1134.

Wang, N., Yuan, Y., Li, Z., Montenbruck, O., & Tan, B. (2015). Determination of differential code biases with multi-GNSS observations. *Journal of Geodesy, 90*(3), 209-228.

Wei, C., Zhang, Q., Fan, L., Zhang, S., Huang, G., & Chen, K. (2014). Estimate DCB of BDS satellites based on the observations of GPS/BDS. *5th China Satellite Navigation Conference, CSNC 2014*, Nanjing, China, May 21-23.

Xue, J., Song, S., & Zhu, W. (2015). Estimation of differential code biases for Beidou navigation system using multi-GNSS observations: How stable are

the differential satellite and receiver code biases? *Journal of Geodesy*, 1-13. doi:10.1007/s00190-015-0874-5.

Yao, Y., Zhang, R., Song, W., Shi, C., & Lou, Y. (2013). An improved approach to model regional ionosphere and accelerate convergence for precise point positioning. *Advances in Space Research*, 52(8), 1406-1415.

Yinhua, L., Xiaohui, L., Jun, R., Huijun, Z., & Lin, Y. (2014). The analysis of Differential Code Bias of BeiDou satellite navigation system. *IEEE International Frequency Control Symposium, IFCS 2014*, Taipei, Taiwan, May 19-22.

Zhang, Q., Zhao, Q., Zhang, H., & Chen, G. (2014). BDS satellites and receivers DCB resolution. *5th China Satellite Navigation Conference, CSNC 2014*, Nanjing, China, May 21-23.

Zhang, R., Song, W.-W., Yao, Y.-B., Shi, C., Lou, Y.-D., & Yi, W.-T. (2015). Modeling regional ionospheric delay with ground-based BeiDou and GPS observations in China. *GPS Solutions, 19*(4), 649-658.

Zhang, S., Chang, X., & Zhang, W. (2013). Real-time regional ionospheric total electron content modeling using spherical harmonic function. *4th China Satellite Navigation Conference, CSNC 2013*, Wuhan, China, May 13-17.

Zumberge, J. F., Heflin, M. B., Jefferson, D. C., Watkins, M. M., & Webb, F. H. (1997). Precise point positioning for the efficient and robust analysis of GPS data from large networks. *Journal of Geophysical Research: Solid Earth, 102*(B3), 5005-5017.

CURRICULUM VITAE

Name Surname: Mohamed Abdelazeem Mostafa MANSOUR

Place and Date of Birth: Aswan, Egypt, 07.10.1984

E-Mail: mostafamansour@itu.edu.tr, moh.azm84@gmail.com

EDUCATION:

June 1, 2014 – May 31, 2015	Ph.D. visiting student, under the joint Ph.D. supervision program, Civil Engineering Department, Ryerson University, Toronto, Ontario, Canada.
November, 2011-June, 2012	Turkish language course (primary, intermediate and advanced), TÖMER, Bursa, Turkey.
November, 2007-March, 2011	M.Sc., Civil Engineering Department, Faculty of Engineering, Aswan University, Aswan, Egypt.
2001-2006	B.Sc., Civil Engineering, Faculty of Engineering, Aswan University, Aswan, Egypt.

AWARDS AND SCHLOARSHIPS:

- Early Career Scientist's Travel Award (ECSTA) supported by the European Geoscience Union (EGU), EGU General Assembly, April 17-22, 2016, Vienna.
- Turkish Government Scholarship for Ph.D. students (2011-2016).
- Egyptian Ministry of Higher Education scholarship for Ph.D. students (2011-2016).

PUBLICATIONS ON THE THESIS:

I. Science Citation Index (SCI) and SCI Expanded papers:

- **Abdelazeem, M.,** Çelik, R. N., & El-Rabbany, A. (2016a). An Enhanced Real-Time Regional Ionospheric Model Using IGS Real-Time Service (IGS-RTS) Products. *Journal of Navigation, 69(3),* 521-530.
- **Abdelazeem, M.,** Çelik, R. N., & El-Rabbany, A. (2016b). An improved regional ionospheric model for single-frequency GNSS users. *Survey Review*, 1-7. doi: 10.1080/00396265.2016.1138581.
- **Abdelazeem M.**, Çelik, R. N., El-Rabbany, A. (2015a). Comparative Study of GPS-TEC Smoothing Techniques. *Acta Geodaetica et Geophysica*, 1-12. doi:10.1007/s40328-015-0153-1
- **Abdelazeem, M.,** Çelik, R. N., & El-Rabbany, A. (2015b). MGR-DCB: A Precise Model for Multi-constellation GNSS Receiver Differential Code Bias. *Journal of Navigation*, 1-11. doi: 10.1017/S0373463315000922.

II. Non-SCI papers:

- **Abdelazeem M.**, Çelik, R. N., El-Rabbany, A. (2015). Regional Ionospheric Delay Correction Model For Single Frequency PPP Users in Turkey. *International Scientific Journal: Micro, Macro, Mezzo Geo Information (MMM-GI)*, No.5, 79-86.

III. Presentations and posters:

- **Abdelazeem M.**, Çelik, R. N., El-Rabbany, A. (2016). A New Model for Real-Time Regional Vertical Total Electron Content and Differential Code Bias Estimation Using IGS Real-Time Service (IGS-RTS) Products. *European Geoscience Union, EGU General Assembly*, Vienna, Austria, April 17-22.
- **Abdelazeem M.**, Çelik, R. N., El-Rabbany, A. (2015). Regional Ionospheric Model for Single Frequency GNSS Users. *123rd Annual General Meeting, Association of Ontario Land Surveyors (AOLS)*, Huntsville, Ontario, Canada, Feburary, 25-27.

OTHER PUBLICATIONS:

- **Abdelazeem, M.**, Çelik, R. N. (2014). Accuracy and Repeatability Investigation of CSRS-PPP Online Processing Service. *Coordinates*, Vol. X (5)**,** 41-49.
- **Abdelazeem, M.,** Farah, A., Farrag, A. F. (2011). Assessment Study of Using Online (CSRS) GPS-PPP Service for Mapping Applications in Egypt. *Journal of Geodetic Science*, 1 (3), 233-239.
- **Abdelazeem, M.,** Farah, A., Farrag, A. F. (2011). Cut-Off Elevation Angle Effect on GPS Positioning Accuracy. *Al-Azhar University Engineering Journal (JAUES),* 5 (1), 565-570.